AD NUMBER

AD846904

LIMITATION CHANGES

TO:

Approved for public release; distribution is unlimited.

FROM:

Distribution authorized to U.S. Gov't. agencies and their contractors; Critical Technology; JAN 1969. Other requests shall be referred to National Aeronautics and Space Administration, Attn: NASA-MSC, EP-2, Houston, TX 77058. This document contains export-controlled technical data.

AUTHORITY

USAEDC ltr, 27 Jun 1973

INVESTIGATION OF COMBUSTION OVERPRESSURE DURING IGNITION OF THE APOLLO BLOCK II SPS ENGINE (AJ10-137) (PHASE VI, PART II)

R. L. Barebo and R. C. Ansley

ARO, Inc.

January 1969

ROCKET TEST FACILITY
ARNOLD ENGINEERING DEVELOPMENT CENTER
AIR FORCE SYSTEMS COMMAND
ARNOLD AIR FORCE STATION, TENNESSEE

NOTICES

When U. S. Government drawings specifications, or other data are used for any purpose other than a definitely related Government procurement operation, the Government thereby incurs no responsibility nor any obligation whatsoever, and the fact that the Government may have formulated, furnished, or in any way supplied the said drawings, specifications, or other data, is not to be regarded by implication or otherwise, or in any manner licensing the holder or any other person or corporation, or conveying any rights or permission to manufacture, use, or sell any patented invention that may in any way be related thereto.

Qualified users may obtain copies of this report from the Defense Documentation Center.

References to named commercial products in this report are not to be considered in any sense as an endorsement of the product by the United States Air Force or the Government.

INVESTIGATION OF COMBUSTION OVERPRESSURE DURING IGNITION OF THE APOLLO BLOCK II SPS ENGINE (AJ10-137) (PHASE VI, PART II)

R. L. Barebo and R. C. Ansley
ARO, Inc.

FOREWORD

The work reported herein was sponsored by the National Aeronautics and Space Administration, Manned Spacecraft Center (NASA-MSC), under Program Area 921E, Project 9281.

The results of research were obtained by ARO, Inc. (a subsidiary of Sverdrup & Parcel and Associates, Inc.), contract operator of the Arnold Engineering Development Center (AEDC), Air Force Systems Command (AFSC), Arnold Air Force Station, Tennessee, under Contract F40600-69-C-0001. The testing was conducted in Propulsion Engine Test Cell (J-3) of the Rocket Test Facility (RTF) between May 27 and June 28, 1968, under Project No. RM1731. This manuscript was submitted for publication on November 5, 1968.

The contents of this report are the results of an altitude testing program to investigate the effects of various starting conditions on the severity of combustion overpressure during ignition of the Aerojet-General Corporation (AGC), Block II AJ10-137, liquid-propellant rocket engine. This testing was included with and interposed between testing for qualification of the engine bipropellant valve (Phase VI).

Technical liaison was provided by AGC, subcontractor of North American Rockwell, Space Division (NAR-SD), for the development of the Apollo Service Module (SM) engine. The test program was requested to support the Apollo project under MIPR-29844G.

Information in this report is embargoed under the Department of State International Traffic in Arms Regulations. This report may be released to foreign governments by departments and agencies of the U. S. Government subject to approval of NASA-MSC (EP-2), or higher authority. Private individuals or firms require a Department of State export license.

This technical report has been reviewed and is approved.

Donald W. Ellison
Lt Colonel, USAF
AF Representative, RTF
Directorate of Test

Roy R. Croy, Jr.
Colonel, USAF
Director of Test

ABSTRACT

An investigation was conducted to determine the magnitude and duration of combustion overpressure during ignition of the Apollo SPS Block II engine. Fifty-four engine starts were made at a pressure altitude of 115,000 ft for a total of 62 sec of firing time. Engine hardware and propellant temperatures were varied from 30 to 70°F but did not influence combustion overpressure. The magnitude of combustion overpressure was affected by propellant injector fill characteristics which were a function of bipropellant valve opening time and target chamber pressure. The overpressure ranged from 0 to 48 percent above the steady-state chamber pressure level for durations ranging from 15 to 39 msec. The overpressure duration was not influenced by the various starting conditions.

CONTENTS

APPENDIXES

I. ILLUSTRATIONS

Figure

SECTION I
INTRODUCTION

The combustion chamber pressure data obtained from Apollo Spacecraft flights 17 and 20 indicated that a momentary combustion overpressure had occurred during the engine ignition transient of the Service Module primary propulsion system. The magnitude and duration of the overpressure reached a level which was considered detrimental to the Command Module/Lunar Module interstage structure of the Apollo vehicle. To ensure the success of future Apollo Spacecraft flights, a ground test program was initiated to determine the magnitude and duration of the combustion overpressure. One engine was used for a total of 54 engine starts. A summary of the individual test periods and test firings is presented in Tables I and II (Appendix II).

The Apollo spacecraft consists of a Command Module (CM, three-man capsule), Service Module (SM) which contains the main propulsion system and propellant tankage, and the Lunar Module (LM). The AJ10-137 rocket engine is the main propulsion engine installed in the SM and, as such, constitutes a major component of the Service Propulsion System (SPS).

Three phases of simulated altitude testing were conducted to develop and qualify the engine (designated the Block I configuration, Refs. 1 through 10), but difficulties encountered during altitude testing and the need for improved performance necessitated further development (Phase IV, Refs. 11 and 12) and qualification testing (Phase V, Ref. 13). The latter engine configuration, designated Block II, was qualified during Phase V testing except for the thrust chamber bipropellant valve (TCV) which developed leaks slightly greater than the specified limits.

Phase VI was instituted primarily for qualification testing of the AJ10-317 engine redesigned TCV, designated Mod I-C. Qualification tests of one Mod I-C TCV were conducted in Phase VI, Part I (Ref. 14). Between qualification tests of two other TCV designs (Mod I-D and Mod I-E), an ignition investigation was conducted and is reported herein.

SECTION II
APPARATUS

2.1 TEST ARTICLE

The Aerojet-General AJ10-137 rocket engine used in the Apollo SPS is a pressure-fed, liquid-propellant engine which includes a self-contained, nitrogen-pressure-actuated bipropellant valve; a doublet impingement injector; an ablative combustion chamber; electric gimbal actuators; and a 62.5:1 area ratio radiation-cooled nozzle extension. The overall height of the complete engine assembly is approximately 13 ft, and the engine assembly weighs approximately 850 lb (Fig. 1, Appendix I). The Block II engine, used for this program, was designed to operate at a nominal 1.60 mixture ratio and a target chamber pressure level of 99 psia for a minimum of 50 starts and an operating life of 750 sec. The liquid, storable, hypergolic propellants were nitrogen tetroxide (N_2O_4) as the oxidizer (MSC-PPD-2A) and Aerozine-50® (AZ-50) as the fuel (MIL-P-27402). The N_2O_4 had a nominal 0.6 percent by weight nitric oxide (NO) additive.

During Phase VI testing, gimbal actuators were not included in the engine assembly; engine gimbal movement was restrained by rigid mechanical linkage. For this ignition investigation, a steel heat-sink-type combustion chamber was used in place of the standard ablatively cooled chamber. The radiation-cooled nozzle extension was attached to the combustion chamber at the 6:1 expansion area ratio. The major components used in this engine assembly were identified as follows:

Engine S/N	055
Chamber (steel) S/N	001
Injector S/N	098
Nozzle Extension S/N	054
TCV (Mod I-D) S/N	DV-4

2.1.1 Combustion Chamber

The combustion chamber was an uncooled, all-steel (type 347 stainless steel), ground test component with the same internal dimensions and contour as the standard flight-type combustion chamber. This steel chamber contained provisions for the installation of several different types of pressure transducers (Fig. 2). The chamber, which had been used by AGC for sea-level tests, was modified by ARO, Inc., to adapt to a standard engine gimbal ring mount and to accommodate the installation of a standard flight-type nozzle extension.

2.1.2 Propellant Injector

Injector S/N 098 was used for a total of 54 starts and approximately 62 sec of firing time during this testing. The injector was a standard Block II flight design (Mod 4) in which the injection orifices were arranged in an impinging doublet configuration. All oxidizer and selected fuel orifices were counterbored to stabilize the injected streams and thereby prevent random chamber pressure pulses (Ref. 13).

2.1.3 Exhaust Nozzle Extension

The radiation-cooled nozzle extension S/N 054 was the standard Block II flight design (columbium-titanium configuration) used previously (Phase V, Ref. 13, and Phase VI, Part I, Ref. 14). Nozzle extension S/N 054 had been tested previously for a total of 3125 sec (Ref. 14) and accumulated approximately 62 sec during this testing, for a total of about 3187 sec of engine firing time. The nozzle acquired some small cracks during previous testing (Ref. 14) but sustained this testing with no further damage because of the short duration firings.

2.1.4 Thrust Chamber Valve and Propellant Lines

The pneumatic pressure-operated, bipropellant valve was a development/nonflight component assembled in the Mod I-D configuration. Gaseous nitrogen stored in two spheres at pressures up to 2500 psia and regulated to approximately 220 psia provided actuation pressure. Electrical command signals were required for opening and closing the valve. The bipropellant valve assembly consisted of eight ball valves: two in each of two parallel fuel passages and two in each of two parallel oxidizer passages (Fig. 3). One fuel passage and one oxidizer passage constituted an independent valve bank; thus the TCV had two valve banks, designated banks A and B. The redundant valve banks allowed normal engine operation if one of the banks should become inoperative in flight. Complete redundancy in the TCV was provided since each of four TCV actuators operated one fuel and one oxidizer ball valve and since one nitrogen sphere and regulator provided pressure for operation of one valve bank. Actuation pressure was supplied through each of two solenoid-operated enable valves to a pair of pilot valves and actuators; thus, valve bank A, bank B, or both banks could be utilized to fire the engine. When only one TCV bank was used, the TCV configuration was referred to as single-bore mode. The TCV was in the dual-bore mode when both TCV banks were operated during a firing.

The TCV was connected to the propellant supply system by the engine propellant lines. The propellant lines contained a flexible bellows section and screen filter at the line inlets. The TCV was connected to the injector by propellant headers which were integral parts of the injector.

Trim orifices were installed at the TCV inlet ports to adjust the pressure losses in the parallel valve passages so that engine operation using either valve bank would produce nearly the same engine performance. Balance orifices were installed at the engine propellant line inlets (interfaces) to adjust the propellant overall pressure losses so that nominal engine operation would result for standard inlet conditions of propellant pressure and temperature. Orifice sizes for all test periods were as follows:

Orifice Diameter, in.						Target Balance Condition
TCV Trim Orifices				Engine Interface Balance Orifices		
Bank A		Bank B				
Oxidizer	Fuel	Oxidizer	Fuel	Oxidizer	Fuel	
1.775	1.475	1.930	1.720	2.800	1.410	Dual Bore

2.1.5 Electric Strip Heaters

Two strip heater pads (Fig. 4) of a prototype spacecraft design were supplied by NAR and were installed on the TCV body by adhesive bonding. Each strip contained an A and a B heating element. The A elements of each pad were connected in parallel as were the B elements to provide two heating circuits of 30-w capacity each. The two circuits could be energized separately or simultaneously.

2.2 TEST CELL INSTALLATIONS

The F-3 fixture and the AJ10-137 engine were installed in the Propulsion Engine Test Cell (J-3), a vertical test cell for testing rocket engines at pressure altitudes of approximately 115,000 ft (Fig. 5 and Ref. 15). A 40-ft-high by 18-ft-diam aluminum test cell capsule, lined with thermopanels to permit temperature conditioning of the cell, was installed over the test article and fixture to form the pressure-sealed test chamber.

The F-3 fixture was a heavy-duty model of the Apollo SPS propellant system which was designed and built by NAR to reproduce the hydrodynamics of the SM spacecraft as closely as practical for ground testing. The spacecraft "zero-g" cans and propellant utilization system were not available for this program. The internal size and shape of the propellant tanks were identical to those of the spacecraft, and the propellant supply lines were identical except for modifications necessitated by ground testing requirements. The Block II tandem arrangement of two tanks was used for each propellant, a 1050-gal sump tank and a 1310-gal storage tank. A schematic diagram of the F-3 fixture is presented in Fig. 6.

A rigid cage structure was installed inside the F-3 fixture, and another inner cage was installed inside the rigid cage. The inner cage was attached to the rigid cage by means of flexure assemblies to permit axial force measurements (Fig. 7). The engine was mounted inside the inner cage.

Two heat shields were installed to protect the instrumentation, the plumbing, and the F-3 fixture from the nozzle extension thermal radiation. One was a facility shield with black Teflon® retained on a sheet steel structure by a steel screen. The second was an NAR-supplied, flight-type, stainless steel shield attached to the combustion chamber/nozzle extension interface.

Pressure altitude was maintained before and after test engine firings with a steam-driven ejector located in the test cell exhaust duct and connected in series with facility exhaust compressors. During the steady-state portion of a firing, pressure altitude was maintained with a supersonic exhaust gas diffuser (Fig. 5).

Additional test facility systems included ground level propellant storage tanks; gaseous helium for F-3 propellant tank pressurization; gaseous nitrogen for test article purging, leak checking, and valve operation; and heat exchangers for temperature conditioning the propellants and the test cell capsule. Equipment for test article operation located in the J-3 control room included the AGC firing console and the combustion stability monitor (CSM).

2.3 INSTRUMENTATION

Instrumentation was provided to measure engine axial force, chamber pressure, temperatures, and accelerations; propellant system pressures, temperatures, and flow rates; and test cell pressures, wall and air temperatures. Instrumentation locations are shown in Figs. 6 and 8.

Instrument output signals were conditioned and recorded variously in (1) frequency form on magnetic tape, (2) digital form on magnetic tape, (3) analog or frequency form on light beam oscillographs, and (4) analog form on indicating/recording null-balance potentiometers with direct-inking paper strip charts, depending on the purpose of the individual parameters.

2.3.1 Pressures

Combustion chamber pressure was measured with three types of transducers in addition to a flight-type transducer which was supplied by NAR. The flight-type transducer was a solid-state silicon wafer strain gage which was installed at the normal injector face tap location with a flight-type "stand-off" mount (Fig. 8b). The other transducers were located on the combustion chamber side walls and were (1) bonded strain-gage types close-coupled with a short nipple for improved response, (2) a flush-mounted, water-cooled, piezoelectric type for highest frequency response and indication of peak pressures, and (3) flush-mounted, water-cooled, variable capacitance types (Fig. 8c).

Propellant pressures and test cell pressure were measured with strain-gage-type transducers. Test cell pressure was also measured by two capacitance-type precision pressure transducers. Except for the piezoelectric type, all transducers were laboratory calibrated prior to installation for this test program with traceability to the National Bureau of Standards (NBS). Before the initial test period all chamber pressure transducers were calibrated off the engine in the test cell in a manner which permitted pressurization and comparison to a secondary standard pressure transducer.

2.3.2 Temperatures

Chromel®-Alumel® (CA) thermocouples were used to measure exterior surface temperatures of the combustion chamber, nozzle extension, injector, TCV, propellant lines and tanks, test cell walls, and test cell air temperature. In addition, propellant temperatures were measured with resistance temperature transducer (RTT) immersion probes, which were laboratory calibrated with traceability to NBS.

2.3.3 Axial Force

Axial force (Fig. 7) was measured with a dual-bridge, strain-gage-type load cell with a rated capacity of 50,000 lb_f. The calibration load cell and data load cell were laboratory calibrated prior to the initial test period with traceability to the NBS. In-place calibration of the

data load cell was accomplished with a hydraulically actuated, axial loading system containing the calibration load cell.

During this test program, the engine gimbal linkage was rigid and included load cells to measure the pitch and yaw forces normally restrained by the actuators.

2.3.4 Propellant Flow Rates

Propellant flow rate measurement was accomplished with one flowmeter in each F-3 fixture propellant feedline upstream of the engine interface (Fig. 6). The flowmeters were turbine-type, axial-flow, volumetric flow sensors with two induction coil signal generators. The flowmeters were calibrated in place with propellants. The calibration techniques are presented in Ref. 16.

2.3.5 Strain

Wire grid strain gages were cemented to the inward and outward surfaces of the engine thrust take-out struts at about the strut midlength points. The gages were provided by AGC and installed on the engine struts by ARO, Inc., while the engine was being built up for testing; therefore, no gage calibration could be made. The manufacturer's gage factors were used for data reduction.

2.3.6 Accelerations

Engine acceleration was measured in three perpendicular planes with piezoelectric-type accelerometers mounted on the injector (Fig. 8a). The output signal of the radial-direction accelerometer was analyzed by the AGC combustion stability monitor (CSM) to initiate engine shutdown automatically in the event of unstable combustion (defined as engine acceleration exceeding 90 g's peak at a frequency of 1200 Hz for longer than 0.080 sec).

SECTION III
PROCEDURE

3.1 TEST ARTICLE BUILD-UP AND HANDLING

Engine components shipped to AEDC for testing had propellant and pneumatic systems internal surfaces in level I (Ref. 17) clean condition. Engine S/N 55 was assembled in the RTF, Class 10,000, Clean Room

(Ref. 15). The buildup of the engine was conducted by ARO, Inc., under the supervision of AGC engineering and quality control personnel. After engine assembly and documentation were completed, the engine was inspected and accepted by ARO, Inc. This engine was then the responsibility of ARO, Inc., until completion of testing.

Prior to installation, the TCV, propellant lines, and thrust chamber were leak checked, and the TCV was functionally checked. After testing was completed, the engine was moved from the test cell to the clean room facilities for disassembly and posttest inspections.

All test hardware was installed and all testing activities were conducted using written procedures. Quality control was maintained throughout this program to ensure that proper procedures were used and that documentation of all activities was accomplished. Surveillance was provided by AGC, NAR, and ARO, Inc.

3.2 PROPELLANTS

Propellant cleanliness requirements for this test (Ref. 17) stated that no particles larger than 500 microns or fibers larger than 1500 by 50 microns shall be present in the propellants. This cleanliness requirement was met in the F-3 Fixture before each test period. In addition, propellant samples were taken to verify that applicable specifications for chemical assay were met.

Additional propellant samples for cleanliness determination were taken approximately midway through each test period during altitude instrumentation calibrations.

3.3 INSTALLATION

During installation in the test cell, leak checks of the facility and F-3 Fixture plumbing were performed. Checkout of the instrument systems was performed. The propellant flowmeters were calibrated in the test configuration using propellants as the flowing media. Mock firings were conducted to ensure that all automatically sequenced events occurred and that the TCV operated satisfactorily. Propellants were conditioned to the test temperature and pumped from ground storage tanks to the F-3 Fixture tanks in the test cell and were again sampled for cleanliness. Calibrations of all pressure, force, and RTT instrumentation were completed at ambient atmospheric pressure. Prior to each test period the test cell capsule was also temperature conditioned.

3.4 TESTING

The test cell was closed and evacuated to approximately 0.4 psia using the facility exhaust compressors. Altitude calibrations of the pressure, force, and RTT instrumentation were conducted, and propellants were bled into the engine. The steam ejector was then used to further reduce the test cell pressure to approximately 0.04 psia, and final temperature conditioning was accomplished with the TCV electric heaters. The required TCV banks were selected manually from the AGC firing console before each firing. The propellant lines were bled in again, and the engine was immediately fired.

The 1-sec firings were controlled using the AGC firing console. The two 4.5-sec-duration firings were initiated and shut down by the facility sequencer. All other firing operations within 60 sec of firing initiation and for 30 sec after shutdown were controlled automatically by the facility sequencer.

Prior to each firing, test article components were temperature conditioned with GN_2 until specified temperature limits or ranges were established as indicated below:

1. During the ambient temperature portion of the program, temperatures of 50 to 90°F were obtained on the TCV and TCV actuators.
2. During the low temperature portion of the program, temperatures of 25 to 35°F were obtained on the TCV and TCV actuators.
3. Prior to all firings, the combustion chamber throat temperatures were decreased to 200°F.

To duplicate a TCV first-start condition (dry TCV) after the first firing of each test period, the propellants were drained from the engine propellant lines; the injector and TCV were purged with GN_2 and then aspirated at 0.4 psia for 10 min. Then propellants were rebled to the upstream ball valves of the TCV prior to the firing. To clean the engine after the final firing of a test period, the injector and TCV were purged with GN_2 and then aspirated at 0.4 psia for 1 hr. Whenever the test cell pressure was above 0.25 psia, a trickle purge of GN_2 was supplied to the injector oxidizer header to provide a dry gas barrier between the ambient atmosphere and the TCV.

3.5 DATA REDUCTION

The ignition transient data were obtained from oscillograms and magnetic tape data converted to oscillograms to provide continuous

analog data for each firing. The primary data obtained during the firings were chamber pressure, oxidizer injector manifold pressure, fuel injector manifold pressure, TCV position traces, and the time at which specific events occurred. Typical start transient oscillograms of these parameters are presented in Fig. 9.

In this report, the following definitions are used,

1. TCV starting condition is referred to as either:
   a. Dry, the condition of the TCV prior to the first engine firing during a space mission, i. e., the TCV is dry -- there are no propellants downstream of the TCV upstream ball valves (Appendix III and Fig. III-1), or
   b. Wet, the condition of the TCV after the first firing. After a firing, a quantity of propellants (both fuel and oxidizer) is trapped between the upstream and downstream ball valves and inside the balls at engine shutdown. This TCV condition is described as wet (Fig. III-1). (The TCV was always in the wet condition except prior to the first firing of each test period and when the propellants were removed from the TCV as described in Section 3.4 prior to an engine firing to provide additional dry start ignition data.)
2. TCV bank selection is referred to as either:
   a. Dual-bore mode, the simultaneous opening of both TCV banks A and B, or
   b. Single-bore mode, the opening of only one TCV bank, either bank A or bank B.
3. TCV opening time is defined as the time required for the ball valve to travel from the full closed position to the full open position (Fig. 9).
4. Target Chamber pressure is used to define the predetermined levels of steady-state chamber pressure corresponding to the selected levels of interface pressures and TCV banks as follows:

Propellant Interface Pressures, psia		TCV Bank Selection	Target Chamber Pressure, psia	
Oxidizer	Fuel			
162 ± 4	169 ± 4	A or B	95	Nominal
162 ± 4	169 ± 4	A and B	99	Nominal
205 ± 4	205 ± 4	A or B	113	High
215 ± 4	215 ± 4	A and B	117	High

5. Chamber pressure rise time is defined as the time from initial TCV open indication to the time at which chamber pressure rose abruptly and approached the steady-state level (Fig. 9, point Ⓒ).

6. Injector manifold fill is defined in Fig. 9 as occurring at point Ⓐ where hydraulic hammer indicates liquid fill of the injector and occurred when the average manifold pressure increased abruptly to the steady-state level. The pressure spikes indicated at point Ⓑ in Fig. 9 are assumed to result from the alternate passage of liquid and gaseous propellant slugs through the injector passages and orifices prior to complete liquid fill.

7. Ignition delay is defined as the time between fuel injector manifold fill and chamber pressure rise.

8. Oxidizer or fuel lead is used to identify which propellant entered the thrust chamber prior to injection of the other propellant.

9. Oxidizer or fuel lead time is defined as the time during which oxidizer or fuel flowed into the chamber ahead of the other propellant.

10. Percent combustion overpressure is defined as follows:

$$\frac{p_{c_{max}} - p_{c_{ss}}}{p_{c_{ss}}} \times 100$$

where: $p_{c_{max}}$ is the maximum chamber pressure; $p_{c_{ss}}$ is the steady-state value. Percent overpressure was calculated for each pressure measurement (Table III) except the measurement from the piezoelectric-type transducer (p_{c_K}) which was a dynamic pressure sensing device and steady-state data were not obtained. The flight-type transducer (p_{c_F}) data were also excluded from overpressure data because the heat sensitivity of the transducer affected the peak and steady-state pressure levels (see Section 4.3).

11. Average percent combustion overpressure was calculated as the average of the chamber pressure data measured by the four pressure transducers located 2.23 in. downstream of the injector-chamber flange. This group consisted of two close-coupled bonded-strain-gage-type transducers (p_{c_6} and p_{c_8}) and two flush-mounted variable-capacitance-type transducers (p_{c_5} and p_{c_7}).

SECTION IV
RESULTS AND DISCUSSION

The combustion chamber pressure data obtained from Apollo Spacecraft flights 17 and 20 indicated that combustion overpressure had occurred during ignition of the AJ10-137 engine. The magnitude and duration of the overpressure had reached a level which was considered detrimental to the CM/LM interstage structure of the Apollo vehicle. To ensure the success of future Apollo Spacecraft flights, the ground test program reported herein was conducted to determine the magnitude and duration of combustion overpressure. To validate the chamber pressure flight data, a flight-type pressure transducer was installed at the same (flight) location on the engine injector, and high-frequency response pressure transducers were installed on the thrust chamber.

The planned test program included one test series with short thrust chamber valve (TCV) opening times (550 to 600 msec) and another with long TCV opening times (750 to 800 msec) to determine the effect of valve opening time on chamber overpressure. The TCV opening times of 500 and 800 msec are the lower and upper design specification limits of the TCV. Each test series was to consist of 30 engine firings of 1-sec duration for the short TCV opening times and 1.5-sec duration for the long TCV opening times with propellants and engine hardware temperature conditioned to 30 and 70°F, with nominal and high target chamber pressure levels, and with the TCV in both the dry and wet condition. However, because of a TCV malfunction, only the short TCV opening times were accomplished during this investigation.

When the TCV is operated in the dual-bore mode, controlling valve sets 1 and 4 (Appendix III) for valve banks A and B, respectively, are orificed to open in approximately equal times. However, during the initial test period at the 30°F temperature conditions (Table I), controlling valve set 4 (Fig. 10) was approximately 300 to 400 msec slower in reaching full open than controlling valve set 1. Subsequently, the valve actuation restrictor orifices were resized to decrease valve opening time and to obtain equal travel times for both controlling valves. During the third test period (Table II) when the propellant and engine hardware temperature were also approximately 30°F, controlling valve set 4 was again slow and exceeded the opening time specification of 550 to 600 msec. The slow valve operation was diagnosed as a mechanical problem resulting from differential thermal expansion at the cold temperatures between the No. 4 actuator piston (Delrin®) and the aluminum cylinder. Since this difficulty could not be remedied in the field, the cold temperature portion of the test series was terminated, and the

remainder of the engine firings were performed at ambient temperature conditions where the proper valve operating time could be obtained. Therefore, the combustion overpressure data obtained during the 30°F temperature dual-bore firings are presented in this report for information only and were not used in the analysis of the ignition characteristics.

4.1 IGNITION CHARACTERISTICS

4.1.1 Chamber Pressure Characteristics

A characteristic common to all chamber pressure traces was the initial low-level pressure activity noted at point Ⓐ on the traces in Fig. 11. This activity varied considerably in its characteristics from a very low-level peak to short duration peaks of as much as 30 percent of steady-state chamber pressure. In some instances, oscillations occurred resembling instability. This chamber pressure activity may be the combustion of propellant vapors forced into the chamber prior to injector liquid fill. No correlations of this activity as to pressure level, time of occurrence or frequency could be made with reference to engine ignition conditions or injector fill characteristics, and it appeared to have no relationship to the severity of overpressure. Accelerations as high as 300 g's were recorded at the time of the initial low-level chamber pressure activity by the three single-axis accelerometers (Fig. 8a) mounted on a boss attached to the engine injector. The accelerations measured at this time during an ignition transient usually exceeded the acceleration recorded at the time of chamber pressure rise (Point Ⓑ in Fig. 11) and did not seem to be compatible with the magnitude of the chamber pressure measured; however, sufficient data were not available for detailed analysis of this phenomenon.

The characteristics of the engine chamber pressure traces varied as a function of TCV bank selection and starting condition. The most distinguishing feature of a dry dual-bore start (Fig. 11a), aside from the high overpressure, was the double peak which occurred for each overpressure. Although it was a distinguishing feature, no conclusions were reached as to the cause. Typical chamber pressure traces of a wet dual-bore start are shown in Fig. 11b. The double peak did not occur, but relatively high overpressures were experienced. Traces of chamber pressure from typical single-bore firings are shown in Figs. 11c and d. The most distinguishing feature of engine starts for these conditions was the occurrence of numerous oscillations in chamber pressure after initial chamber pressure rise (Region Ⓒ in Figs. 11c and d).

During the analysis of the ignition data, it was observed that variations in the starting conditions affected the propellant injector manifold fill characteristics which in turn were the direct cause for the variations in combustion overpressure. Therefore, it was necessary to determine the effect of these variables on injector fill time first to understand the resultant effect on combustion overpressure. These variables were (1) TCV opening time, (2) TCV starting condition, (3) TCV bank selection, (4) target chamber pressure, and (5) propellant and injector temperatures.

4.1.2 Effect of TCV Opening Time

The effect of TCV opening time on injector manifold fill times is shown in Fig. 12. It can be seen that both oxidizer and fuel injector fill times increased as TCV opening time increased, irrespective of TCV starting condition, TCV bank selection, or target chamber pressure. The shorter fill times resulting from a faster opening TCV were caused by the higher initial propellant flow rate during injector fill. The momentary increase in propellant flow rate was indicated by both the fuel and oxidizer flowmeter data.

The effect of injector manifold fill time on combustion overpressure is presented in Fig. 13. These data indicate a decrease in combustion overpressure with an increase in injector manifold fill time. Instrumentation difficulties prevented the acquisition of the injector fill data during test periods FM and FN. Therefore, the data presented in Fig. 13 were obtained only during test period FO, which had engine ignitions with only short TCV opening times (500 to 600 msec).

The effect of increased injector fill times was to delay chamber pressure rise. The chamber pressure rise time as a function of TCV opening time is shown in Fig. 14. As would be expected, these data indicate the same general trend as exhibited by the injector fill time data.

Since the injector manifold fill time was a direct function of TCV opening time, and because of limited injector manifold fill data, TCV opening time data were used to further illustrate the effect of injector manifold fill time on combustion overpressure. To obtain a wider range of TCV opening times, it was necessary to use combustion overpressure data acquired during a previous test series (Ref. 18) where the TCV banks operated properly at longer opening times between 700 and 800 msec. These data were obtained using the same type of thrust chamber valve and one high-response-type chamber pressure transducer installed on the injector. However, the overpressure data at the longer TCV opening times (Ref. 18) were obtained at propellant

and engine hardware temperatures of 30°F as compared with a temperature of 70°F for the short valve opening times obtained during this investigation. To isolate the temperature effect from the valve opening time effect, overpressure was plotted as a function of propellant temperature for constant TCV opening times (Fig. 15). These data indicate little or no temperature effect on overpressure over the range of propellant temperatures from 30 to 70°F.

Combustion overpressure as a function of TCV opening time is presented in Fig. 16. These data indicate a decrease of approximately 20 percent in combustion overpressure for dual-bore starts when TCV opening time was increased (or an increased injector fill time) from 500 to 800 msec. For single-bore starts and the same TCV opening time span, average combustion overpressure decreased 8 percent for bank A and approximately 3 to 4 percent for bank B (Fig. 16b).

The duration of the combustion overpressure was not influenced by TCV opening time (Fig. 17). When the TCV was operated in the dual-bore mode, the overpressure duration was approximately 3 to 8 msec longer than that measured during single-bore operation. The average overpressure duration (an average of the overpressure duration measured by pressure transducers p_{c5}, p_{c6}, p_{c7}, and p_{c8}) for 70 percent of all engine firings was between 20 and 30 msec. Eighteen percent of the overpressure durations were between 30 and 40 msec, and the remaining 10 percent were below 20 msec (Table IV).

4.1.3 Effect of TCV Bank Selection and TCV Starting Condition

The data presented in Figs. 12 and 14 indicated that the fuel and oxidizer fill times and the time to chamber pressure rise were longer when operating in the single-bore mode as compared with dual-bore mode. This results from the fact that in the single-bore mode, the total valve opening area is only one-half that of the dual-bore mode. Therefore, single-bore pressure drop is greater, which results in lower propellant flow rates and thus longer fill times. The data also indicated that the TCV start condition had little or no influence on injector fill time except for dual-bore starts. During the dual-bore starts, fuel fill time occurred later during the ignition transient when the TCV was in the dry condition as compared with the wet condition (Appendix III).

In Fig. 18, it can be seen that, during wet dual-bore starts, the oxidizer and fuel fill times were approximately the same. However, during dry dual-bore starts, fuel fill times were substantially longer than the oxidizer fill times. This effect resulted in oxidizer manifold fill prior to both fuel injector fill and chamber pressure rise, resulting

in an oxidizer lead and a combustion overpressure greater than 20 percent (Fig. 19). In the case of single-bore operation, the oxidizer injector manifold apparently fills substantially slower, and oxidizer fill did not occur until after both fuel fill and chamber pressure rise had occurred; this results in an apparent fuel lead and combustion overpressures less than 20 percent (Fig. 19). Although some of the single-bore start data indicated an increase in the fuel lead when the TCV was in the wet condition as compared with the dry condition, sufficient data were not available to confirm this trend. The fuel lead resulted in numerous chamber pressure spikes during the ignition transient as shown in Region © in Figs. 11c and d. The mechanism by which the variation in propellant lead time affects chamber overpressure was concluded to be that an oxidizer lead results in a more efficient propellant mixture ratio at ignition than is the case during simultaneous injection or fuel lead.

For the same starting conditions (and similar TCV opening times), the overpressure measured during a dry dual-bore start was about 30 percent higher than during a dry single-bore start (Fig. 19). The wet dual-bore starts were approximately 15 percent higher than the wet single-bore starts. The highest overpressure measured during this investigation occurred when the TCV was operated dry in the dual-bore mode. There was little or no difference in the overpressure measured during single-bore starts regardless of the TCV bank selection at similar starting conditions.

4.1.4 Effect of Target Chamber Pressure

Target chamber pressure for dual-bore operation had no measurable influence on injector manifold fill times. The same is true for single-bore operation (Fig. 12). However, the average percent combustion overpressure decreased with an increase in target chamber pressure for a constant valve opening time (Fig. 16). The overpressure was approximately 10 percent higher at the target chamber pressures of 95 and 99 psia as compared with the target chamber pressures of 113 and 117 psia for both dual-bore and single-bore starts. Although the percent of overpressure was less during the high target chamber pressure firings, the magnitude of the peak pressure during the overpressure was in general much higher (Table III). Peak chamber pressures of approximately 170 psia were measured during two high chamber pressure level firings.

4.1.5 Effect on Ignition Delay

Although the relationship of fuel and oxidizer fill times varied with the conditions mentioned, ignition delay, the time between fuel fill and chamber pressure rise, was consistent at an average of approximately 6 msec and apparently was unaffected by the many variables.

4.1.6 Combustion Overpressure Data Statistics

Seventy-five percent of all TCV dual-bore starts at propellant engine hardware temperatures near 70°F had average overpressures greater than 20 percent (Table IV). During the ignition of two of these starts, combustion overpressures above 40 percent were observed. The largest overpressure (47.9 percent) occurred when the engine was operating at 99-psia target chamber pressure, and the other large overpressure (40 percent) occurred at 117-psia target chamber pressure. The TCV was in the dry condition prior to the ignition for both engine firings. In addition, all engine firings conducted at 99-psia target chamber pressure, dual-bore mode, and at ambient temperature resulted in an overpressure greater than 20 percent. Only one TCV single-bore start (approximately 5 percent of all single-bore starts) resulted in an overpressure greater than 20 percent. An overpressure of 25.5 percent was observed when TCV Bank A was utilized at propellant and engine hardware temperatures near 30°F with the TCV dry.

The average combustion overpressure frequency distribution is shown below:

Average Percent Combustion Overpressure	Percent of Total Number of Engine Firings Conducted
40 to 50	5.3
30 to 40	18.4
20 to 30	10.5
0 to 20	55.8

(These data do not include the chamber overpressure data obtained during engine firings where the TCV was operating improperly in the dual-bore mode at propellant temperatures near 30°F.)

4.2 CHAMBER PRESSURE SPIKES

The occurrence of pressure spikes or overpressures of short duration ($\leq$ 5 msec) was noted during the different phases of engine operation.

Conditions affecting the occurrence of these pressure spikes could not be identified, but their occurrence was unusual enough to warrant documentation in this report. These pressure spikes occurred during four separate phases of engine operation: (1) the ignition transient, (2) steady-state operation, (3) the shutdown transient, and (4) after engine shutdown. These pressure spikes did not exceed approximately 75 percent of steady-state chamber pressure, and their occurrence was verified by all chamber pressure measurements and by measured accelerations of generally low level (< 300 g's). Typical examples of each of these pressure spikes are shown in Fig. 20. Pressure spikes during phases 1, 3, and 4 occurred randomly throughout the test program; however, pressure spikes for phase 2 were not detected prior to the fifth engine firing of the last test period which was the 33rd firing in the total series of 54 firings.

4.3 FLIGHT-TYPE TRANSDUCER EVALUATION

The peak chamber pressure measured with the variable-capacitance-type transducer agreed well with the peak pressure measured with bonded strain-gage-type transducer (Fig. 21a). The data indicate that the variable-capacitance-type transducer data were consistently 5 to 10 psia higher than the bonded strain-gage-type transducer data. This trend in the data was expected because the frequency response of the variable-capacitance-type transducers exceeds that of the bonded strain-gage-type transducers. However, the measurements of chamber pressure recorded by the flight-type transducer did not agree with the other pressure transducer measurements obtained during this investigation. In Fig. 21b, the magnitude of the peak chamber pressure measured with the flight-type transducer is compared with average data obtained from two variable-capacitance-type pressure transducers. For the majority of engine firings, the flight-type transducer indicated a higher peak pressure than did the other pressure transducer. The peak chamber pressure measured with the flight-type transducer varied from 40 psia above to 45 psia below the peak pressure measured by the variable-capacitance-type transducers. This effect was aggravated when the initial test article temperature was near 30°F. Although the flight-type transducer was mounted on a stand-off (Fig. 8c) which in turn was connected to a drilled passage through the injector, there was very little difference in response between the flight-type transducer data and that measured directly on the chamber wall (Fig. 21c).

In addition, it was noted that the transducer indicated a varying pressure during the initial steady-state portion of the firings as shown in Fig. 22. This anomaly occurred during approximately 75 percent of the engine firings. All other pressure transducers indicated that a

steady-state chamber pressure had been reached approximately 100 to 150 msec after combustion overpressure had occurred (Fig. 9).

Previous NAR test experience with this type of transducer at the White Sands facilities indicated that the flight-type transducer was heat sensitive. The standoff used for the flight-type transducer installation at AEDC was incorporated first by NAR at White Sands to reduce this heat sensitivity. The poor agreement of the flight-type transducer chamber pressure data with the other transducer data for both the peak pressures and the initial steady-state levels is believed to result from thermal gradients across the transducer caused by the hot combustion gases during the ignition transient.

4.4 ENGINE HARDWARE DAMAGE

A visual inspection of the injector after the test series revealed that the diameter of several oxidizer orifices, located inside the area of the cylindrical baffle (Fig. 23), had been enlarged. An enlargement of the photograph of the damaged area is shown in Fig. 23b. Some orifice diameters had been enlarged more than others, and the surface surrounding these orifices was also deformed (bulged) in the outward direction. Since the damage was localized and occurred only to the counterbored oxidizer orifices, the thickness of the injector face at these orifices could have been less than the thickness of the other oxidizer orifices. Normal cyclic pressurization during the test series could have caused the orifices to gradually become deformed. Another possible cause was that a localized overpressurization in the injector passages occurred during some of the firings. However, the instrumentation needed to determine the cause of this anomaly was not installed on the injector. Since the damage to the injector was small and possibly a gradual process, the effect on engine performance could not be detected. Combustion efficiency (c*) calculated from two 4.5-sec firings conducted during the test series was normal. One of these two firings was the final firing of the test series.

Other engine hardware damage consisted of small holes found in the fuel filter located at the engine fuel interface (Fig. 24). These holes were located where the screen was welded to the downstream stiffener. A visual inspection of the damage indicated that the screen could have been damaged or made brittle by welding during manufacture, and through normal cyclic pressurization, metal fatigue occurred. This is somewhat substantiated by the fact that the filter had been slightly deformed in the outward direction during the test series. Damage or deformation of the oxidizer filter located at the corresponding oxidizer interface could not be detected by visual inspection.

SECTION V
SUMMARY OF RESULTS

The results of the combustion overpressure investigation of the Apollo Block II SPS Engine (AJ10-137) in the J-3 test cell are summarized as follows:

1. The combustion overpressure ranged from 0 to 48 percent above the steady-state chamber pressure level.
2. The combustion overpressure duration was not influenced by the various starting conditions. Seventy percent of all the firings had an overpressure duration between 20 and 30 msec. Eighteen percent of the overpressure durations was between 30 and 40 msec, and the remaining 10 percent was below 20 msec.
3. The magnitude of the peak chamber pressure measured with the flight-type transducer did not agree with data obtained from the other pressure transducers. It was surmised that heat sensitivity of the flight transducer caused the transducer to indicate a higher peak pressure and also a varying pressure during the steady-state portion of the firings.
4. Propellant and injector temperature did not significantly influence combustion overpressure over the range of temperature investigated (30 to 70°F).
5. An increase in TCV opening time resulted in an increase in injector fill times which decreased combustion overpressure. When the TCV opening time was increased from 500 to 800 msec, the overpressure decreased approximately 20 percent for dual-bore starts. For single-bore starts and the same TCV opening time span, average combustion overpressure decreased 8 percent for bank A and approximately 3 to 4 percent for bank B.
6. The difference in injector fill characteristics during dual-bore and single-bore starts caused an oxidizer lead to occur during the dual-bore starts and a fuel lead to occur during single-bore starts. The overpressure measured during the dry dual-bore starts was about 30 percent higher than for the dry single-bore starts. The overpressure for the wet dual-bore starts was approximately 15 percent higher than for the wet single-bore starts.

7. Combustion overpressure was approximately 10 percent higher at the 99-psia target chamber pressure than at the 117-psia target chamber pressure for dual-bore mode starts. An identical increase in overpressure with decrease in target chamber pressure was observed during single-bore mode firings.

REFERENCES

1. DeFord, J. F. "Simulated Altitude Testing of the Aerojet-General Corporation AJ10-137 Rocket Engine (Report I - Phase I Development Test)." AEDC-TDR-64-81 (AD350408), May 1964.
2. McIlveen, M. W. "Simulated Altitude Testing of the Aerojet-General Corporation AJ10-137 Rocket Engine (Report II - Phase I Development Test)." AEDC-TDR-64-82 (AD350407), May 1964.
3. Vetter, N. R. and DeFord, J. F. "Simulated Altitude Testing of the Aerojet-General Corporation AJ10-137 Rocket Engine (Report III - Phase I Development Test)." AEDC-TDR-64-146 (AD352141), July 1964.
4. McIlveen, M. W. "Simulated Altitude Testing of the Aerojet-General Corporation AJ10-137 Rocket Engine (Report IV - Phase I Development Test)." AEDC-TDR-64-147 (AD352327), August 1964.
5. Vetter, N. R. and DeFord, J. F. "Simulated Altitude Testing of the Aerojet-General Corporation AJ10-137 Rocket Engine (Report V - Phase I Development Test)." AEDC-TDR-64-158 (AD352700), August 1964.
6. Vetter, N. R. and McIlveen, M. W. "Simulated Altitude Testing of the Aerojet-General Corporation AJ10-137 Rocket Engine (Report VI - Phase I Development Test)." AEDC-TDR-64-171 (AD352933), September 1964.
7. Schulz, G. H. and DeFord, J. F. "Simulated Altitude Testing of the Apollo Service Module Propulsion System (Report I - Phase II Development Test)." AEDC-TR-65-233 (AD368743), January 1966.
8. Robinson, C. E. and Runyan, R. B. "Thrust Vector Determination for the Apollo Service Module Propulsion Engine using a Six-Component Force Balance." AEDC-TR-65-250 (AD475564), December 1965.

9. Schulz, G. H. and DeFord, J. F. "Simulated Altitude Testing of the Apollo Service Module Propulsion System (Report II - Phase II Development Test)." AEDC-TR-66-17 (AD369807), February 1966.

10. Gall, E. S., McIlveen, M. W., and Berg, A. L. "Qualification Testing of the Block I Apollo AJ10-137 Service Module Engine." AEDC-TR-66-129 (AD374879), August 1966.

11. Pelton, J. M. and McIlveen, M. W. "Block II AJ10-137 Apollo Service Module Engine Test at Simulated High Altitude (Report I - Phase IV Development)." AEDC-TR-66-169 (AD376952L), November 1966.

12. DeFord, J. F., McIlveen, M. W., and Berg, A. L. "Block II AJ10-137 Apollo Service Module Engine Testing at Simulated High Altitude (Report II - Phase IV Development)." AEDC-TR-67-47 (AD812441), April 1967.

13. Gall, E. S., McIlveen, M. W., and Berg, A. L. "Qualification Tests of the Apollo Block II Service Module Engine (AJ10-137)." AEDC-TR-67-63 (AD813868), May 1967.

14. Schulz, G. H., Berg, A. L., and Robinson, C. E. "Apollo Block II SPS Engine (AJ10-137) Environmental Tests and Mod I-C Bipropellant Valve Qualification Tests (Phase VI, Part I)." AEDC-TR-68-178 (AD842097), October 1968.

15. Test Facilities Handbook (Seventh Edition). "Rocket Test Facility, Vol. 2." Arnold Engineering Development Center, July 1968.

16. Berg, A. L. "Rocket Propellant Inplace Flowmeter Calibration System - Propulsion Engine Test Cell (J-3)." AEDC-TR-68-41 (AD833157), May 1968.

17. Aerojet-General Corporation Specification AGC-46848A "Engine, AJ10-137 (Apollo), Altitude Qualification Test Procedure for." March 17, 1967.

18. Farrow, K. L., Berg, A. L., and Robinson, C. E. "Apollo Block II SPS Engine (AJ10-137) Mod I-D and Mod I-E Bipropellant Valves Qualification Tests (Phase VI, Part III)." AEDC-TR-69-7 (to be published).

APPENDIXES

I. ILLUSTRATIONS
II. TABLES
III. DESCRIPTION OF THRUST CHAMBER VALVE (TCV) OPERATION

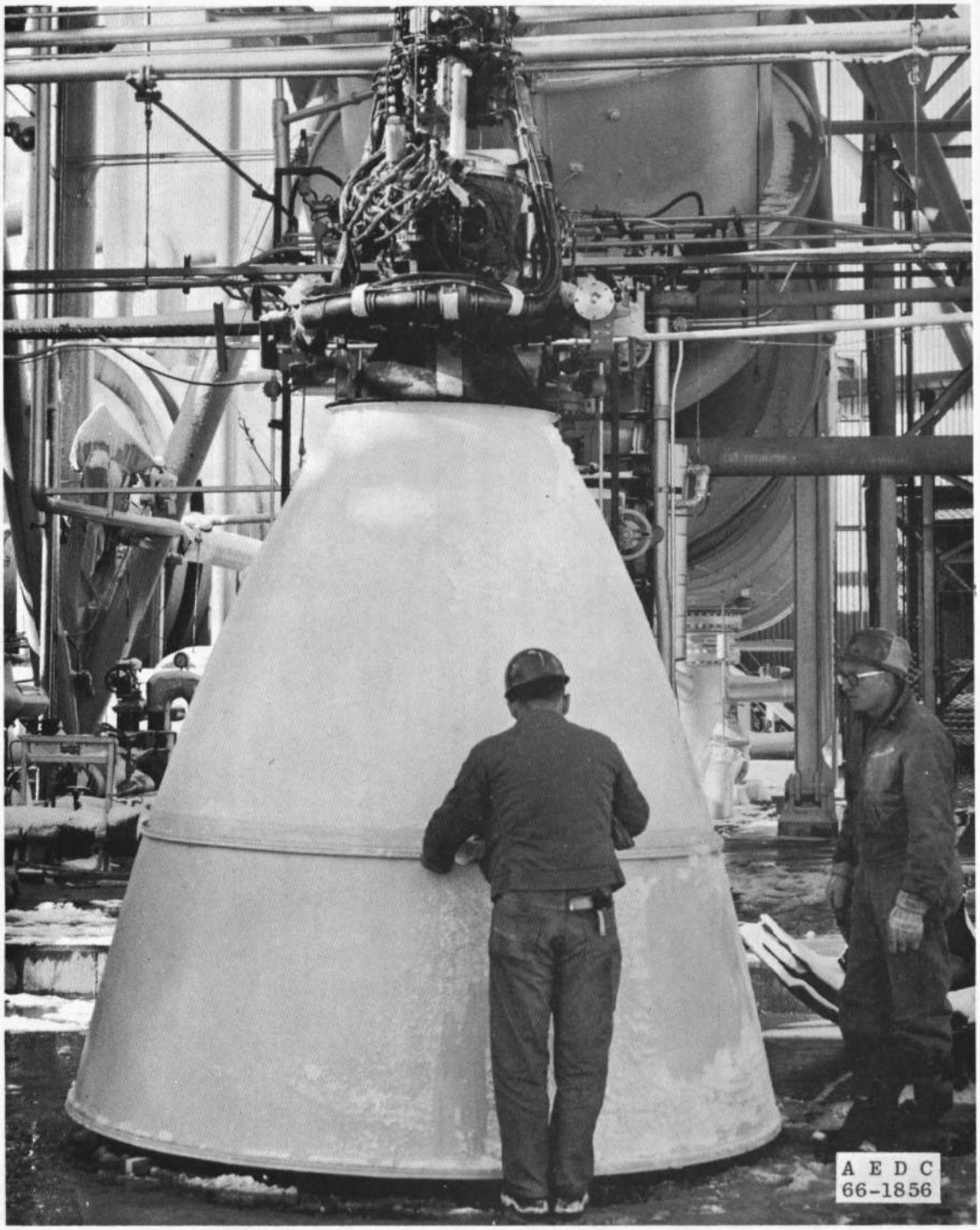

Fig. 1 The Apollo SPS Block II Engine

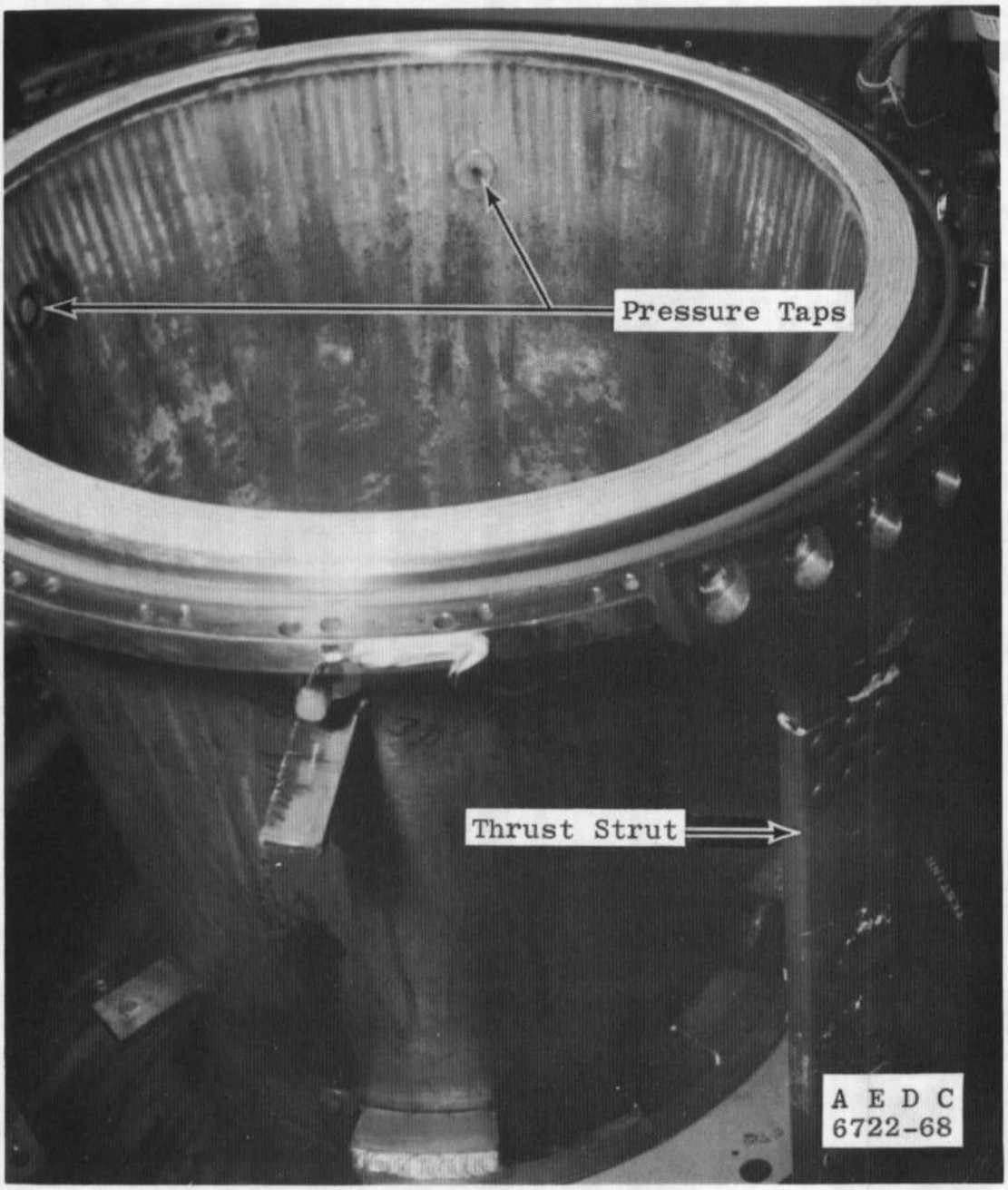

a. Injector Attachment Flange

Fig. 2 The All-Steel Combustion Chamber

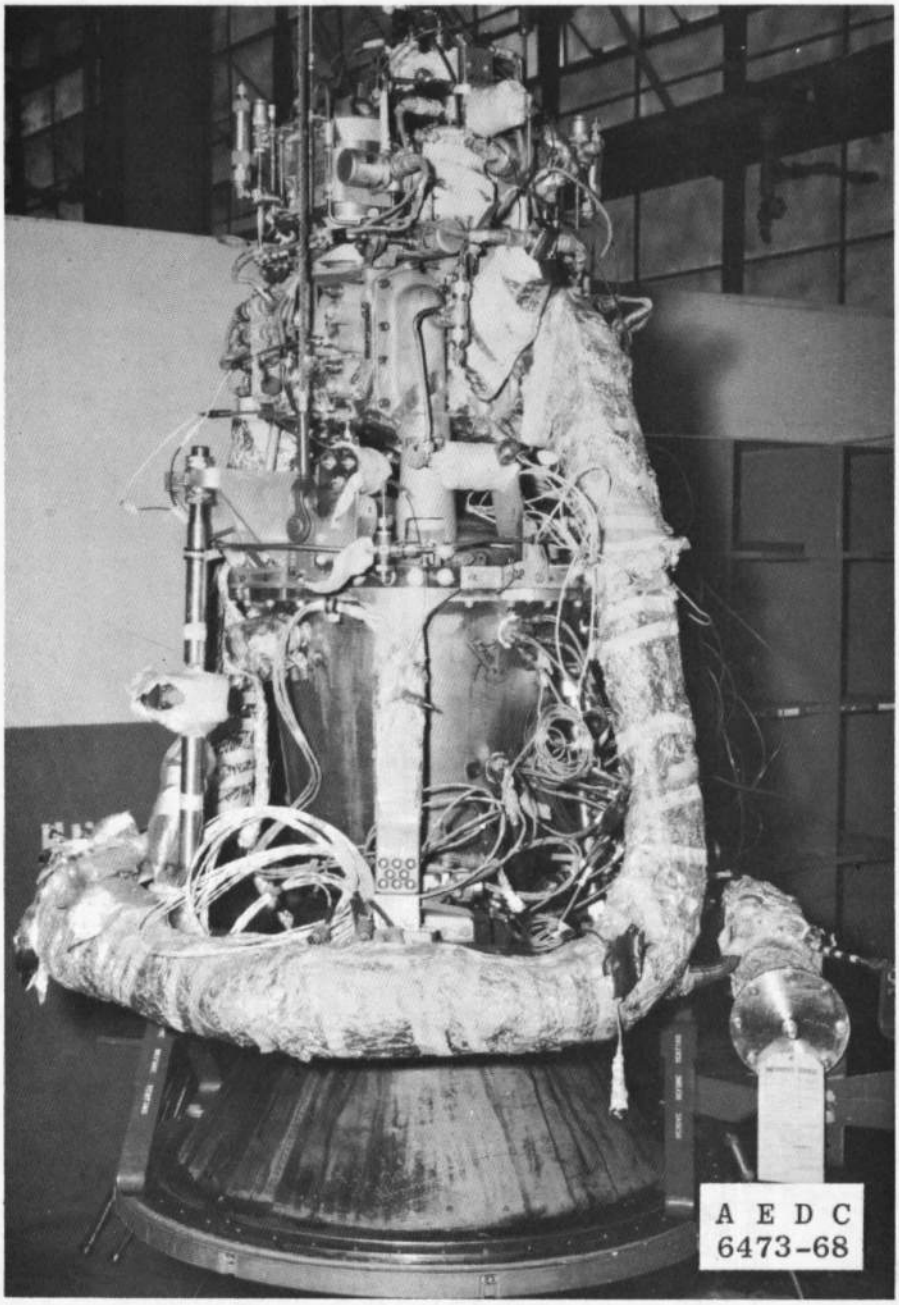

b. Installation on the SPS Engine

Fig. 2 Concluded

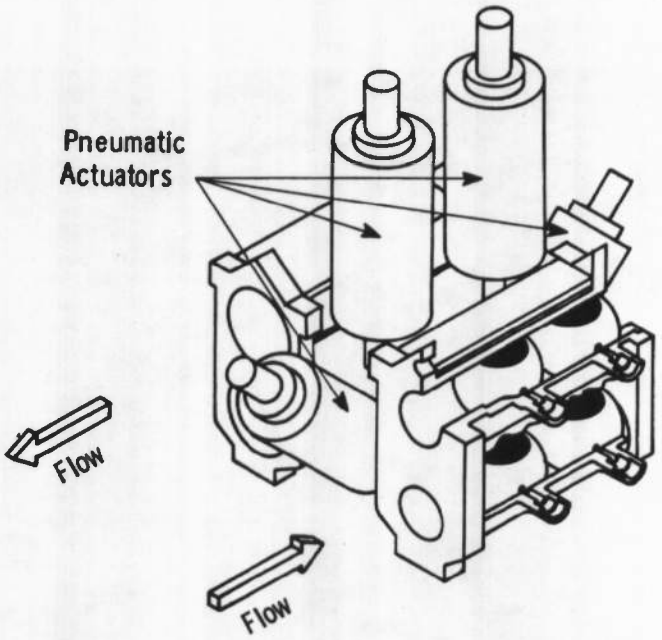

a. General Arrangement

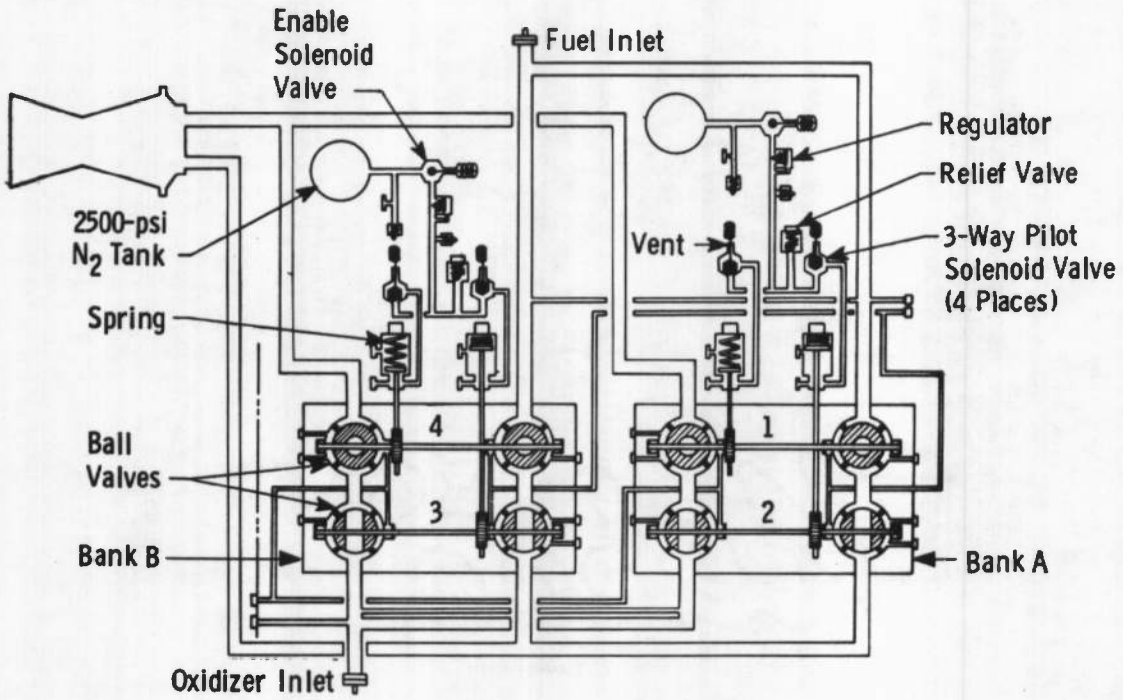

b. Flow Diagram

Fig. 3 Block II Thrust Chamber Valve (Bipropellant)

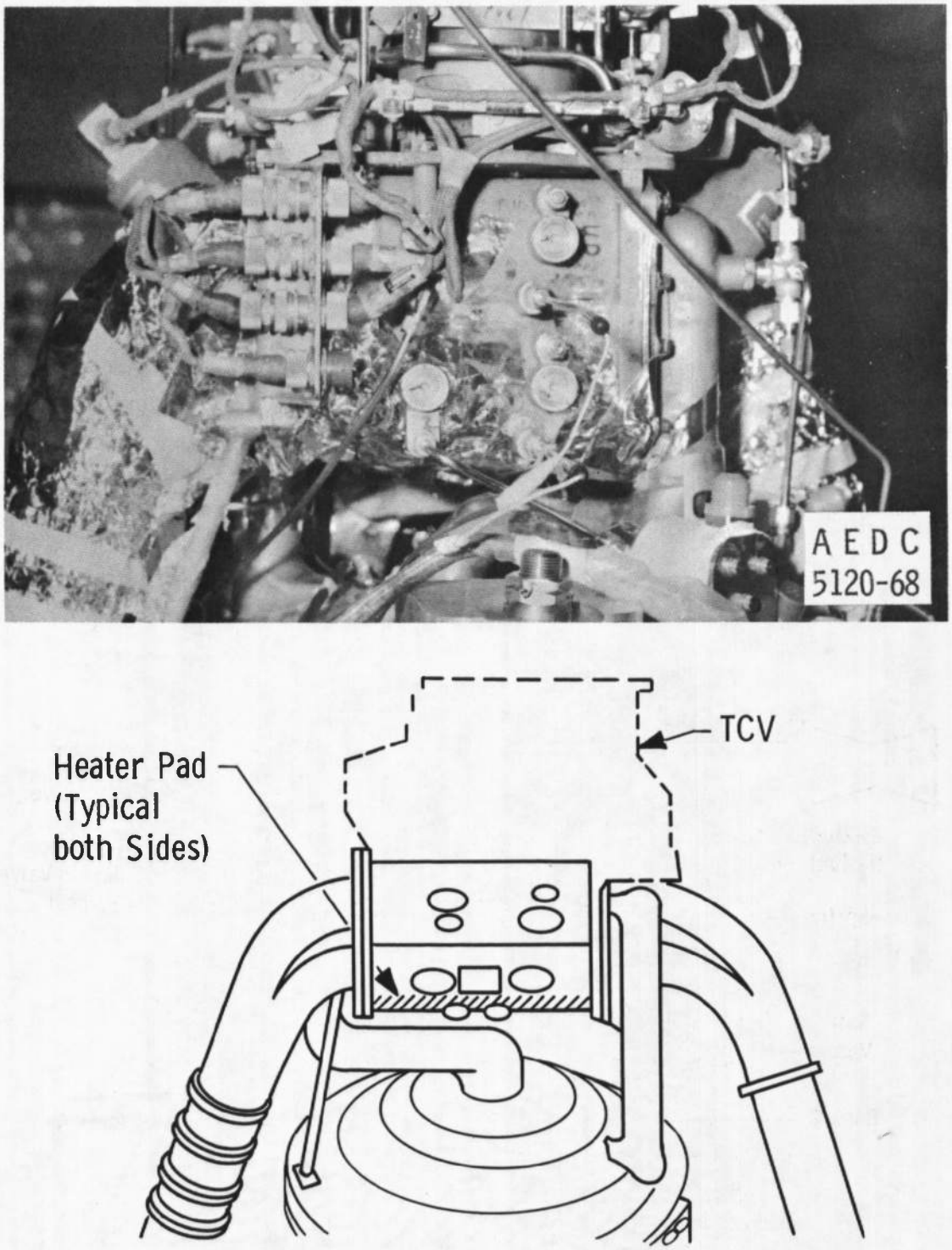

Fig. 4 Thrust Chamber Valve Strip Heaters

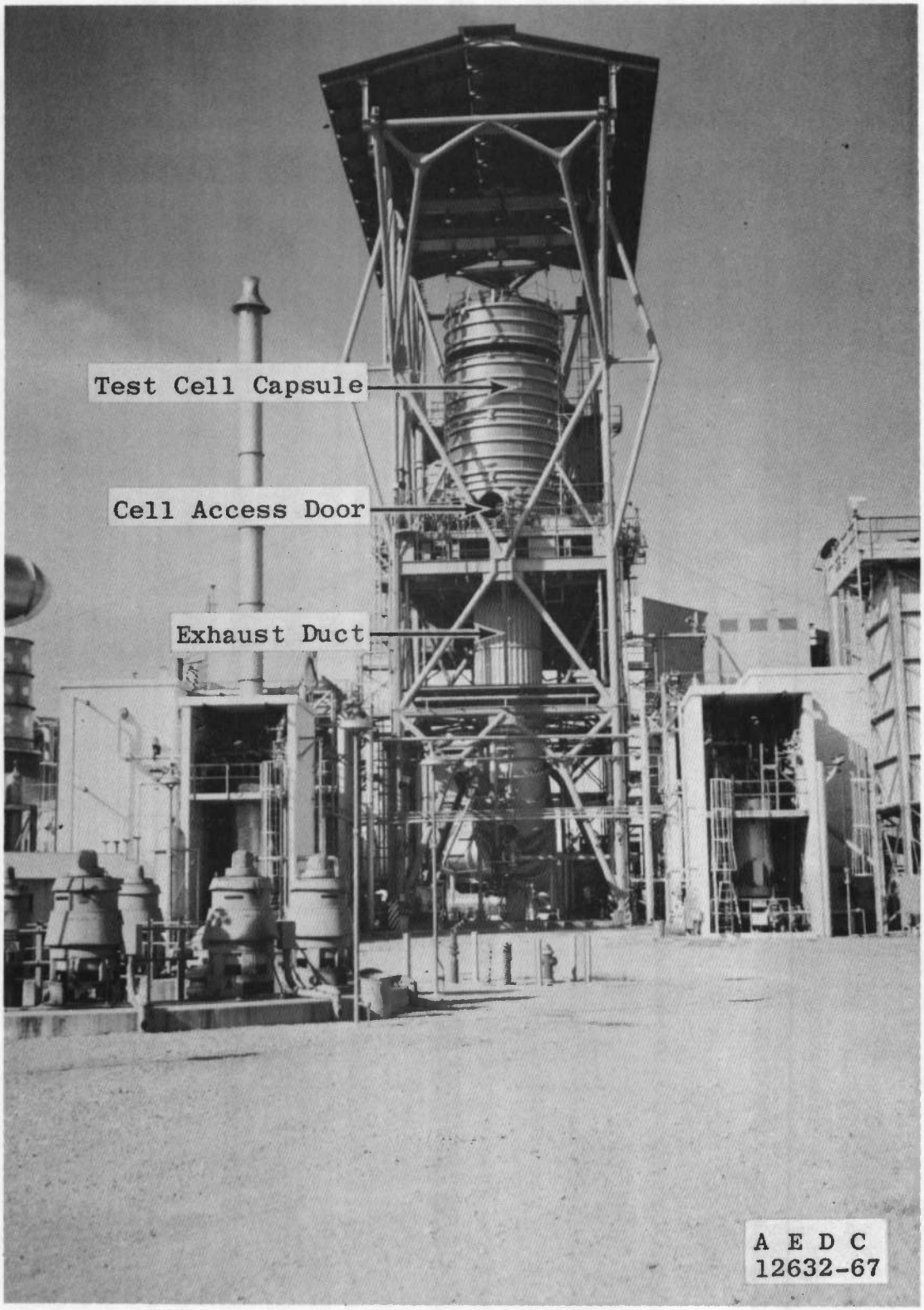

a. Complex

Fig. 5 Propulsion Engine Test Cell (J-3)

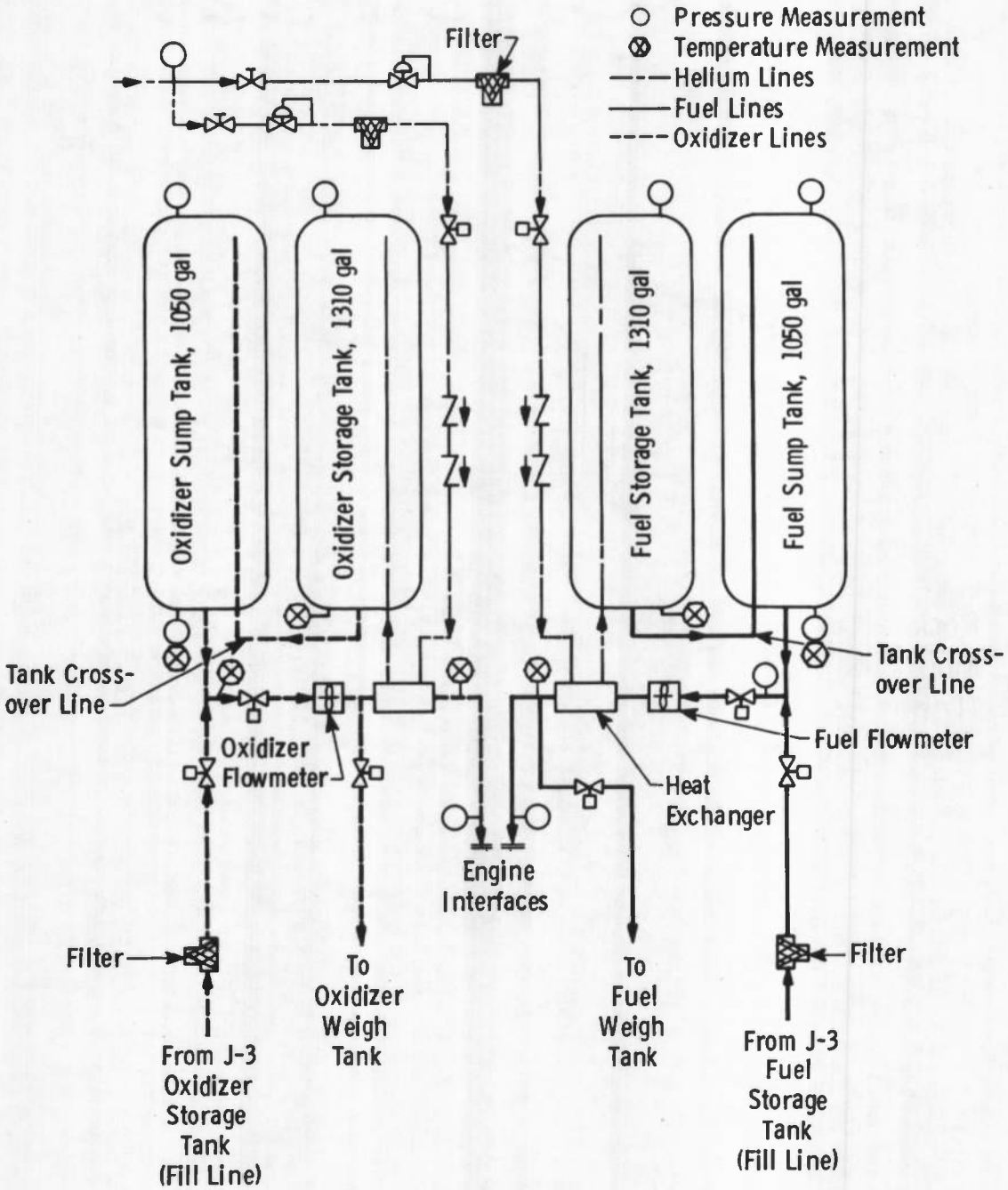

Fig. 6 Schematic of the F-3 Fixture

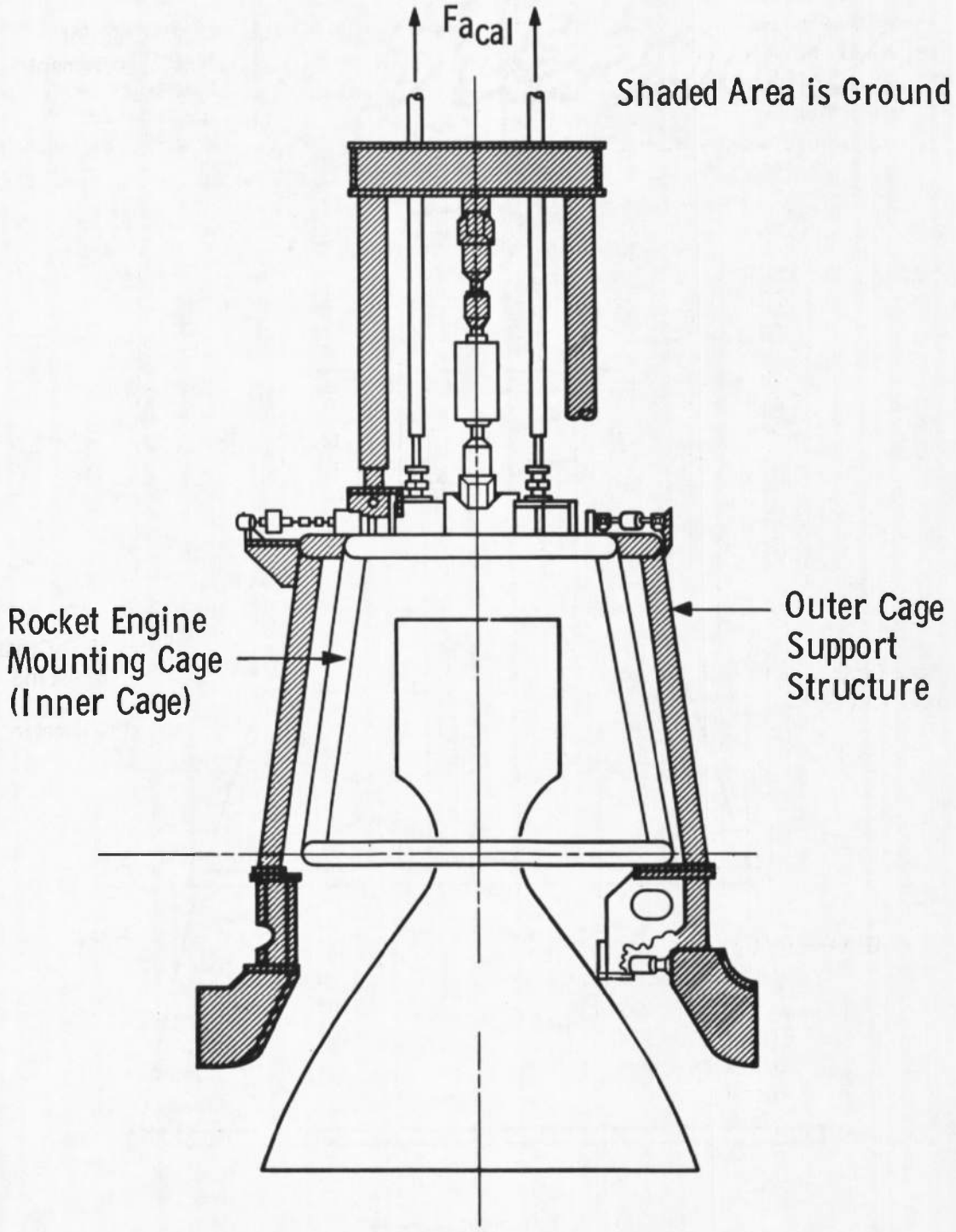

Fig. 7 Arrangement of the Thrust System

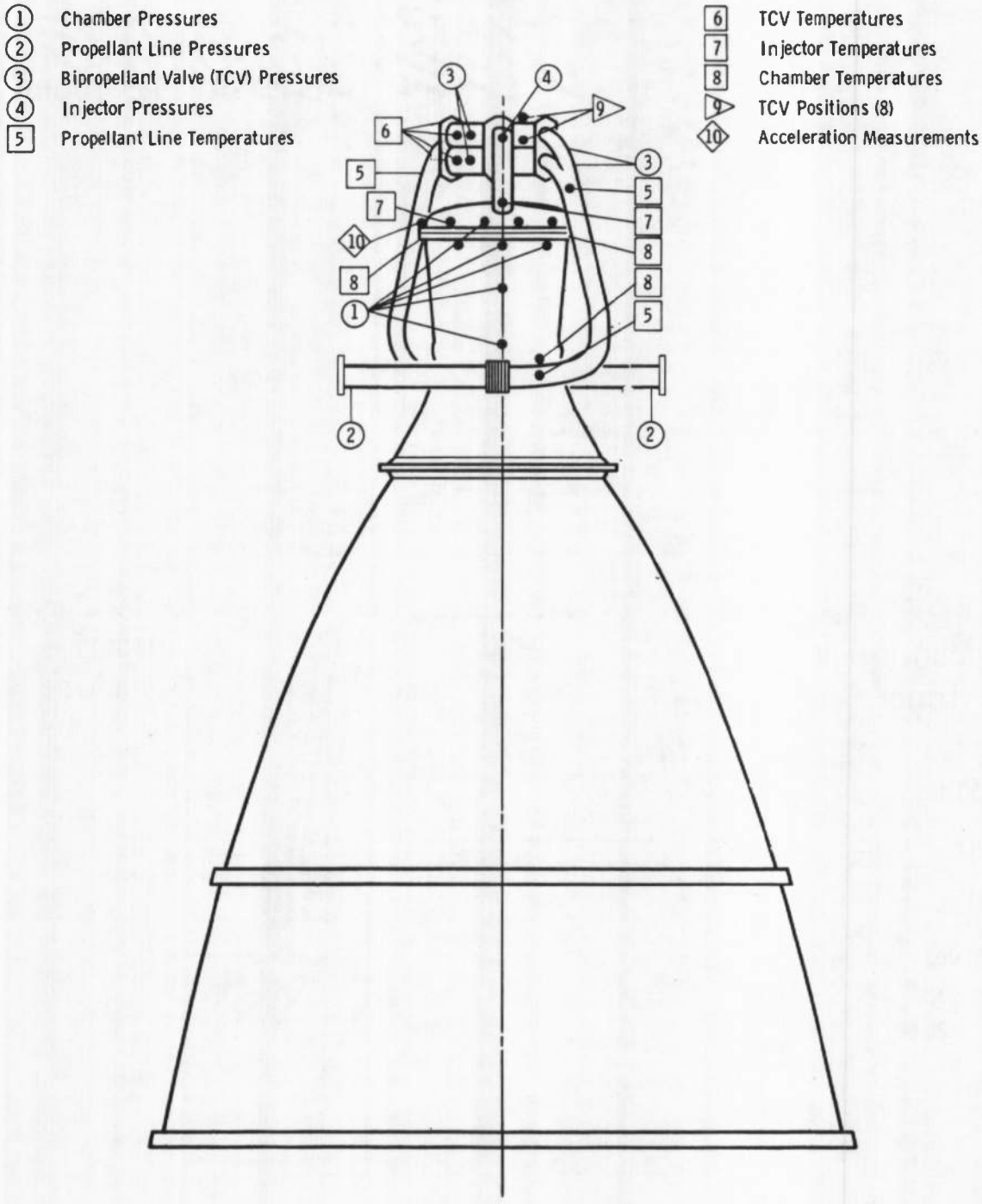

a. General Locations

Fig. 8 Engine Instrumentation Locations

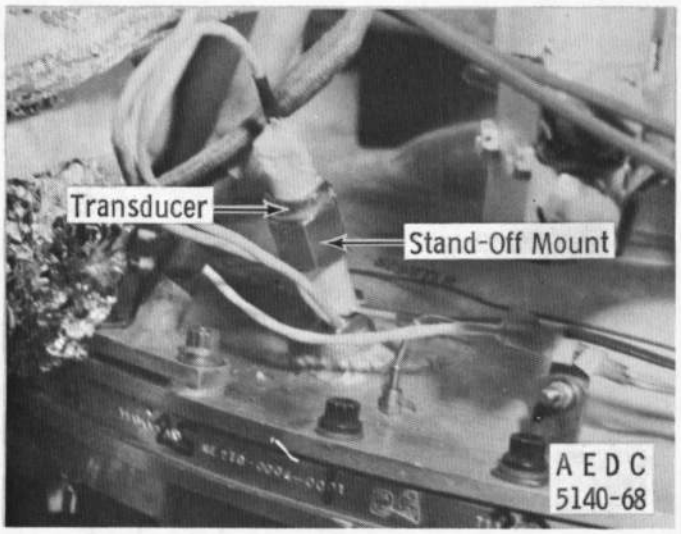

b. Flight-Type Transducer Installation

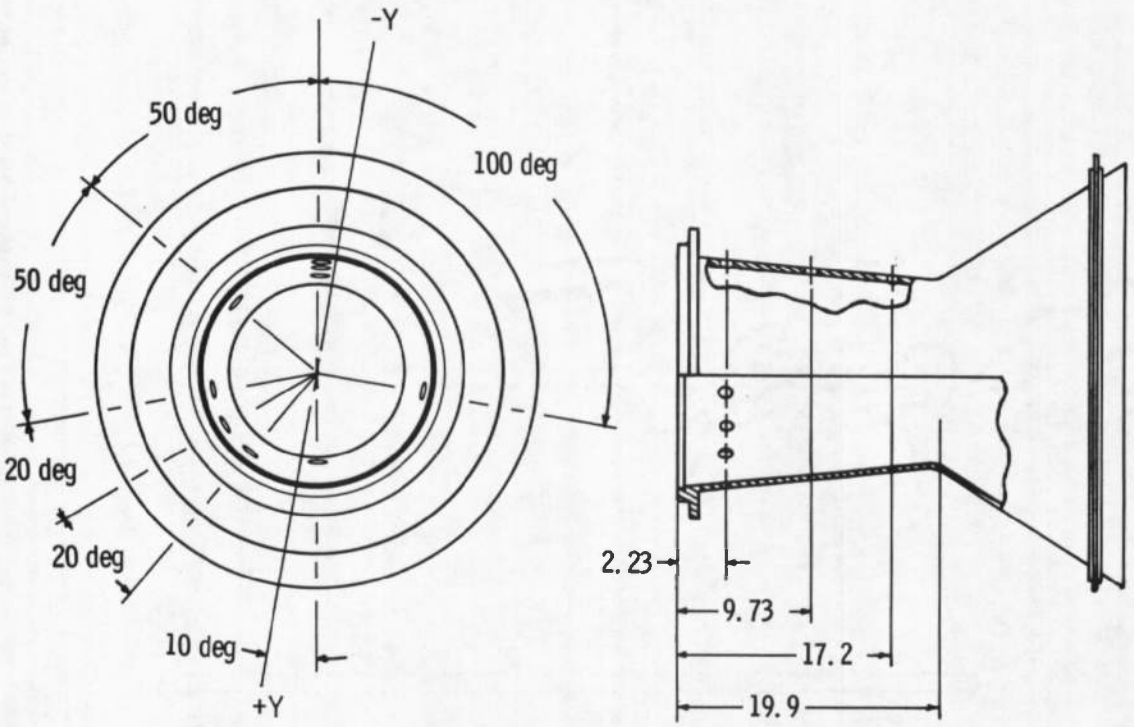

c. Chamber Pressure Transducer Locations

Fig. 8 Concluded

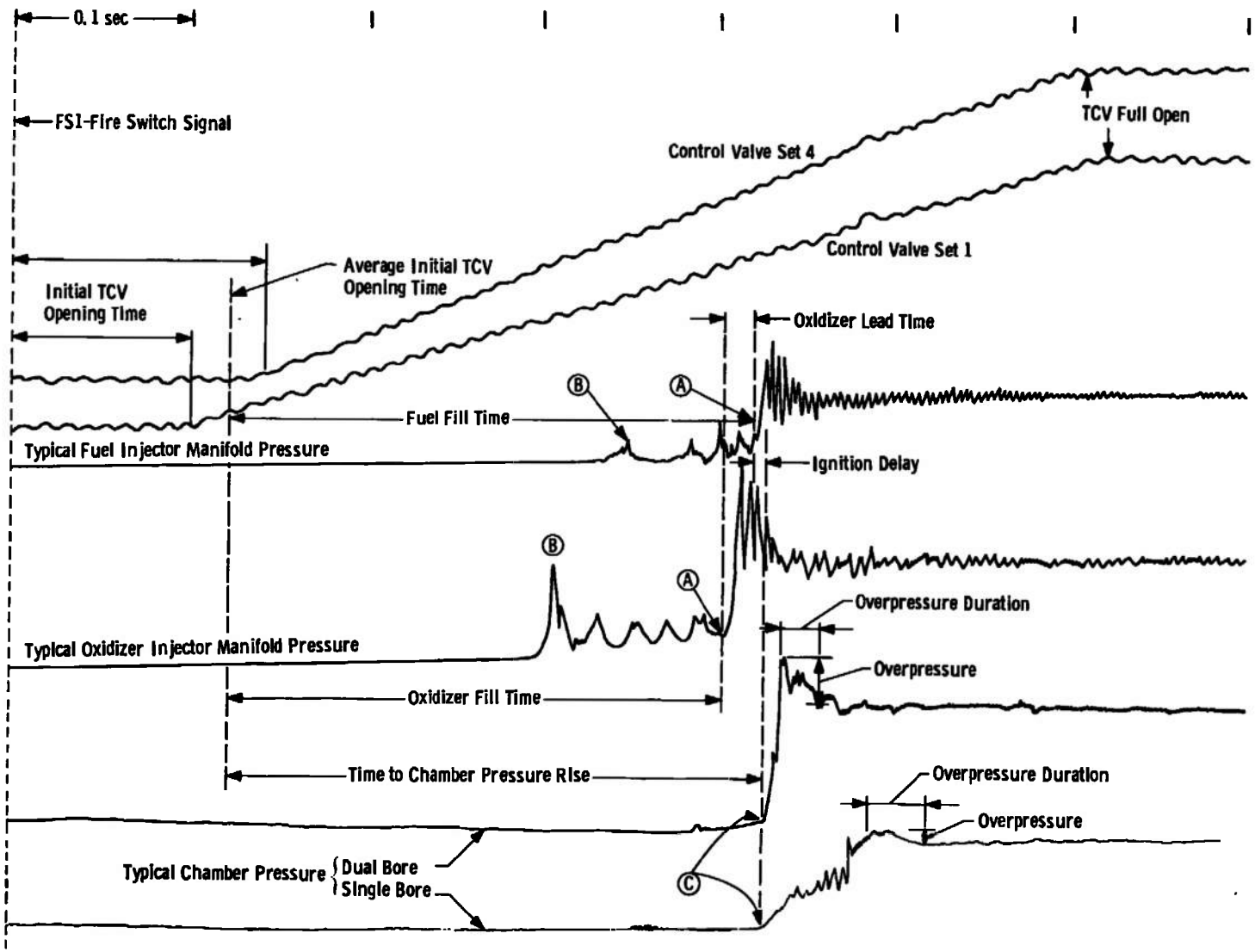

Fig. 9 Typical Start Transient Oscillograms

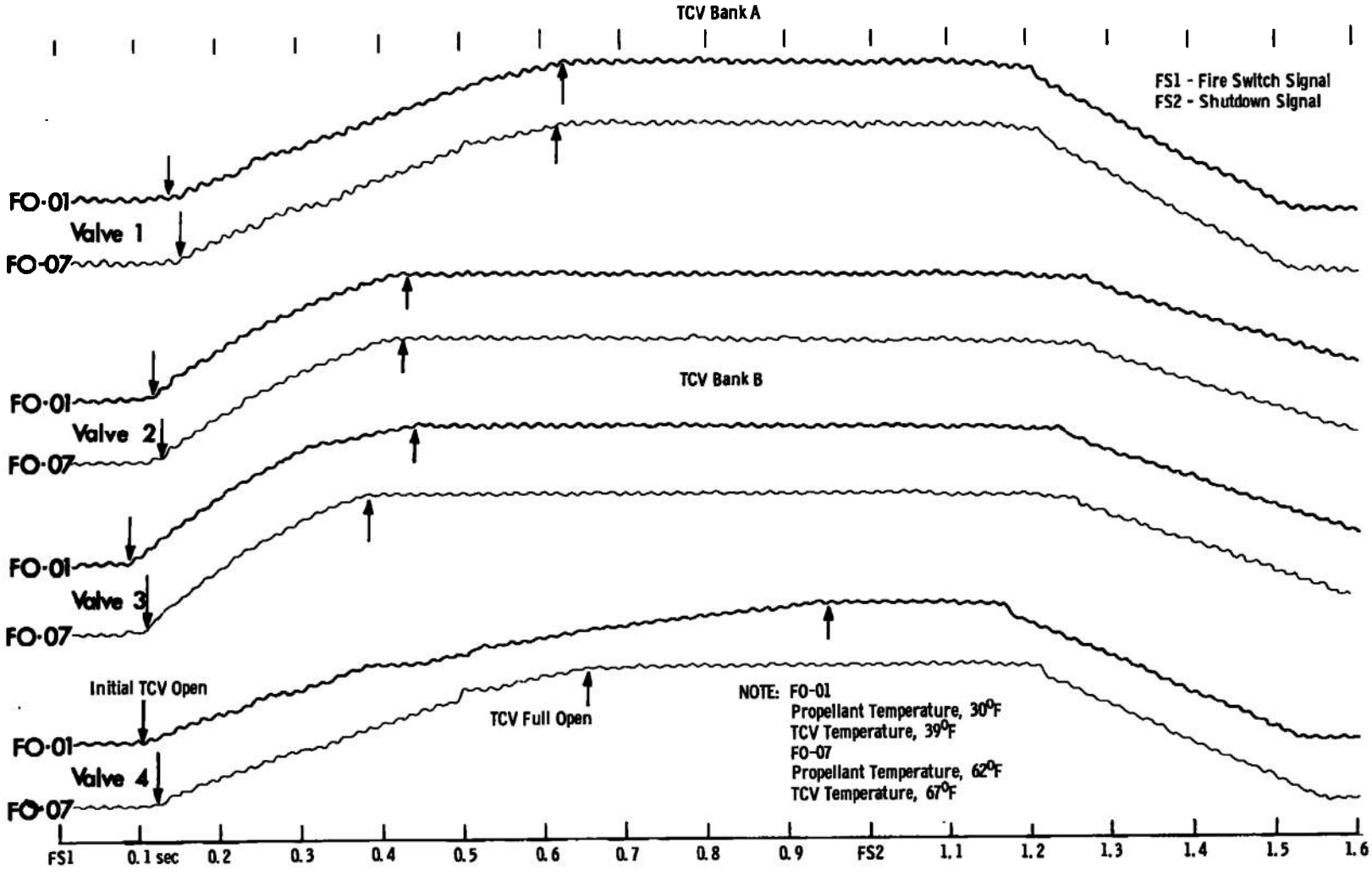

Fig. 10 Typical TCV Opening Oscillograms

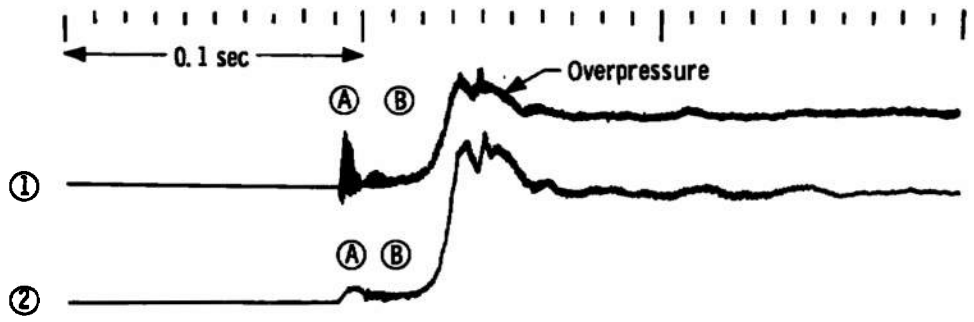

a. Dry Dual-Bore Start

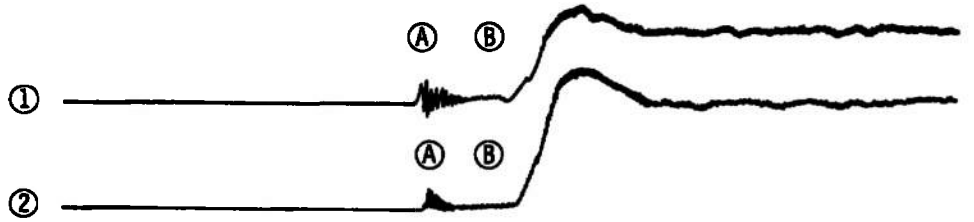

b. Wet Dual-Bore Start

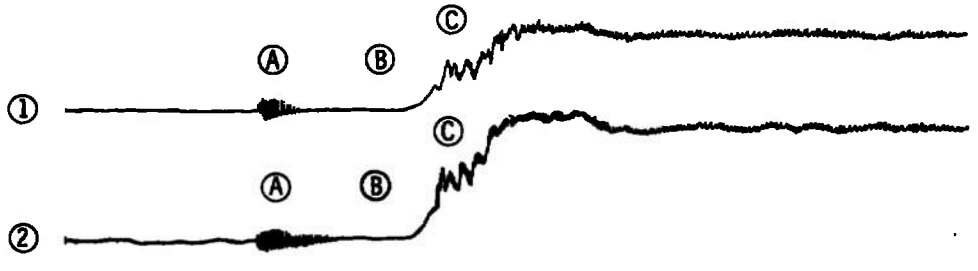

c. Dry Single-Bore Start

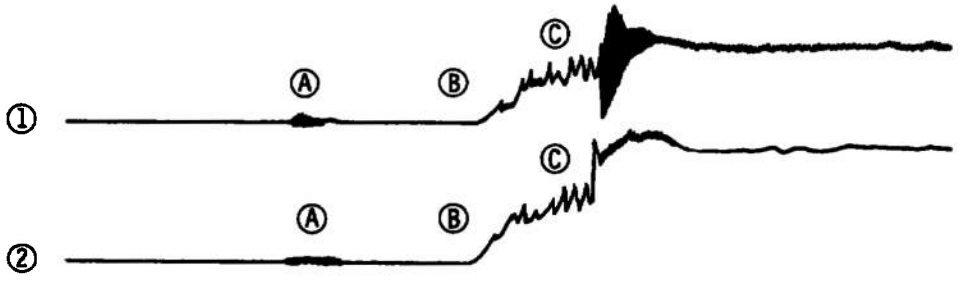

d. Wet Single-Bore Start

Fig. 11 Typical Chamber Pressure Oscillograms

① Chamber Pressure Measured by a Bonded-Strain-Gage-Type Transducer

② Chamber Pressure Measured by a Variable-Capacitance-Type Transducer

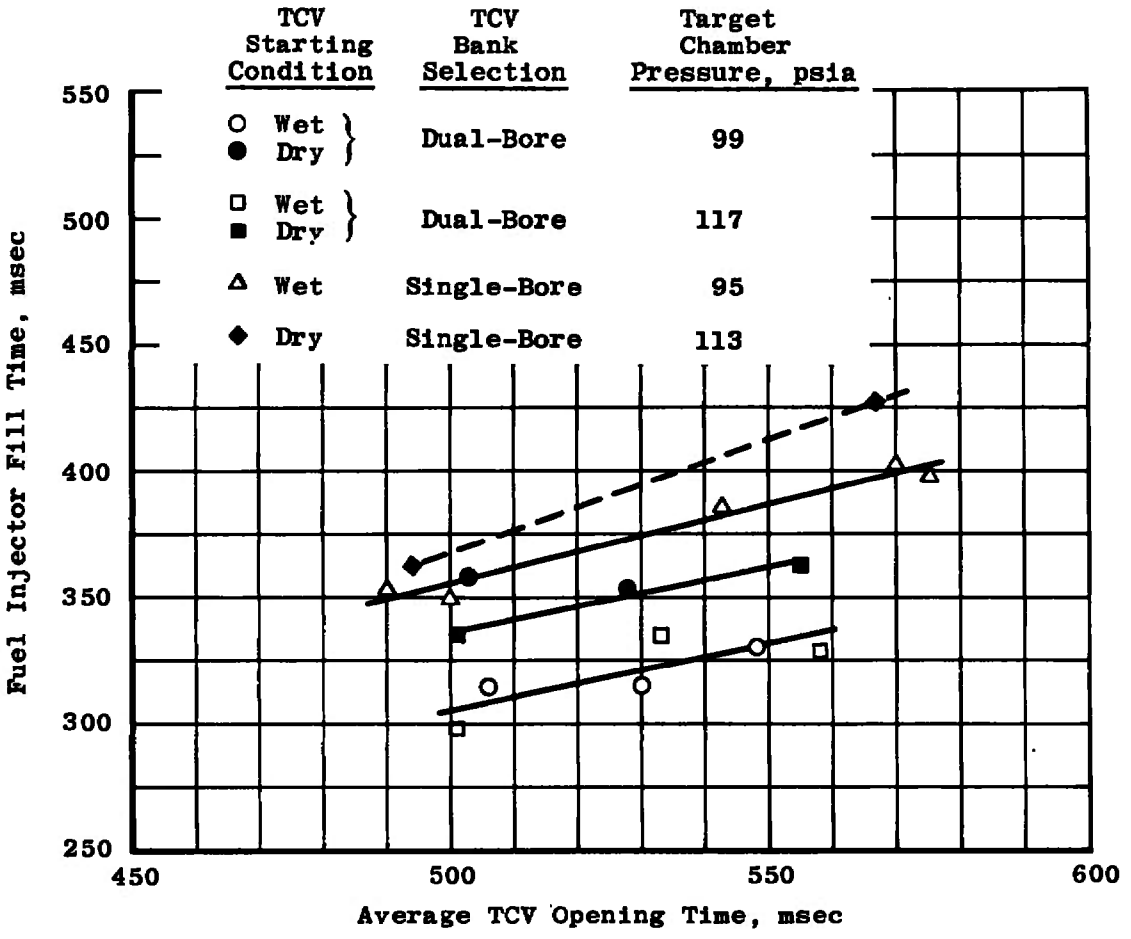

a. Fuel Injector

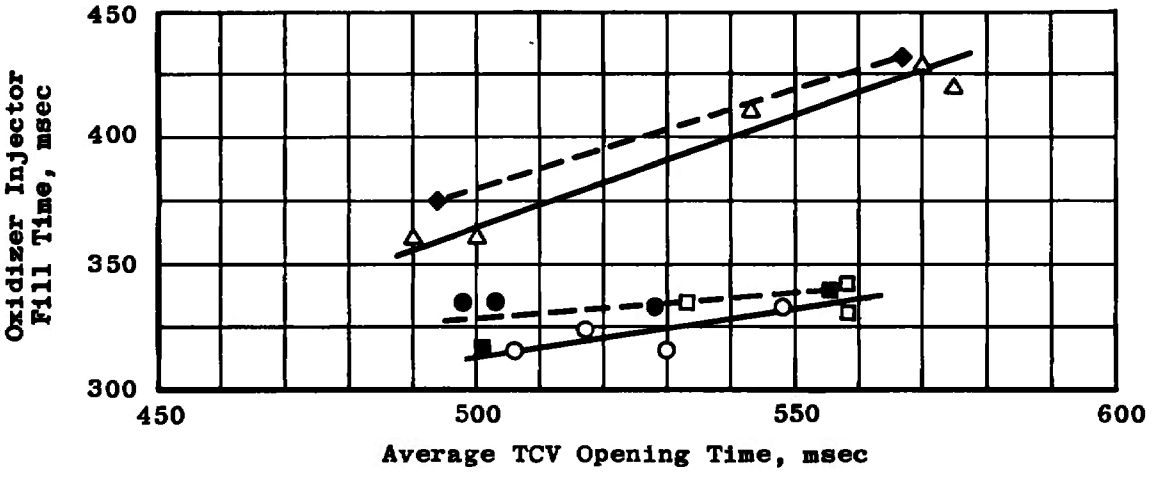

b. Oxidizer Injector

Fig. 12 Injector Manifold Fill Time as a Function of TCV Opening Time

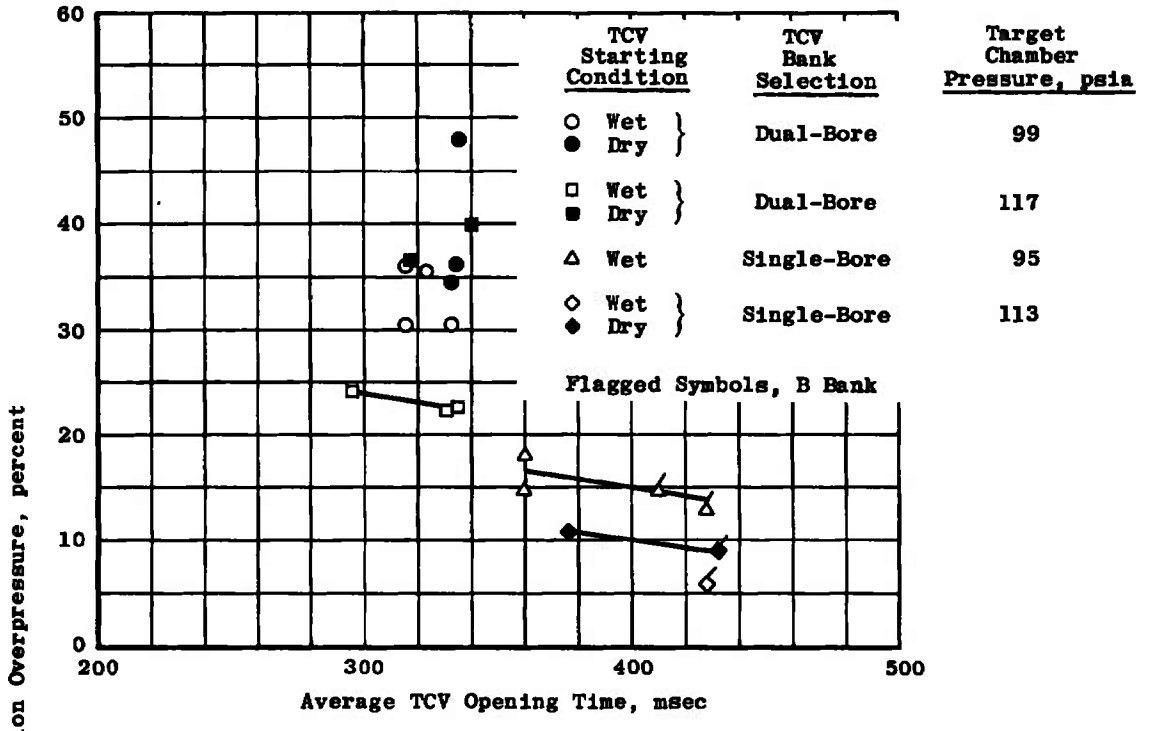

a. Oxidizer Injector

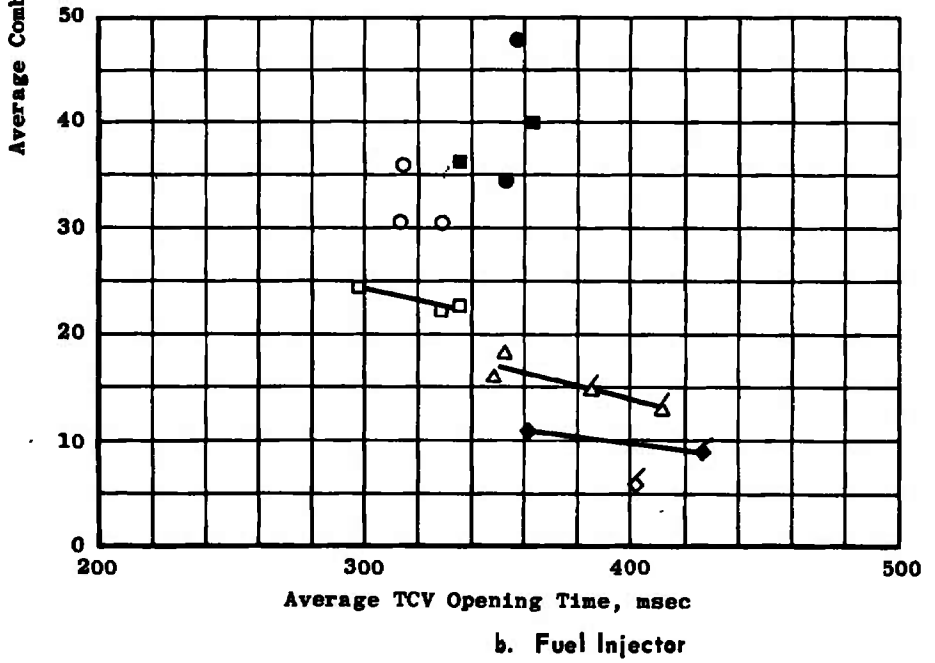

b. Fuel Injector

Fig. 13 Average Combustion Overpressure as a Function of Injector Manifold Fill Time

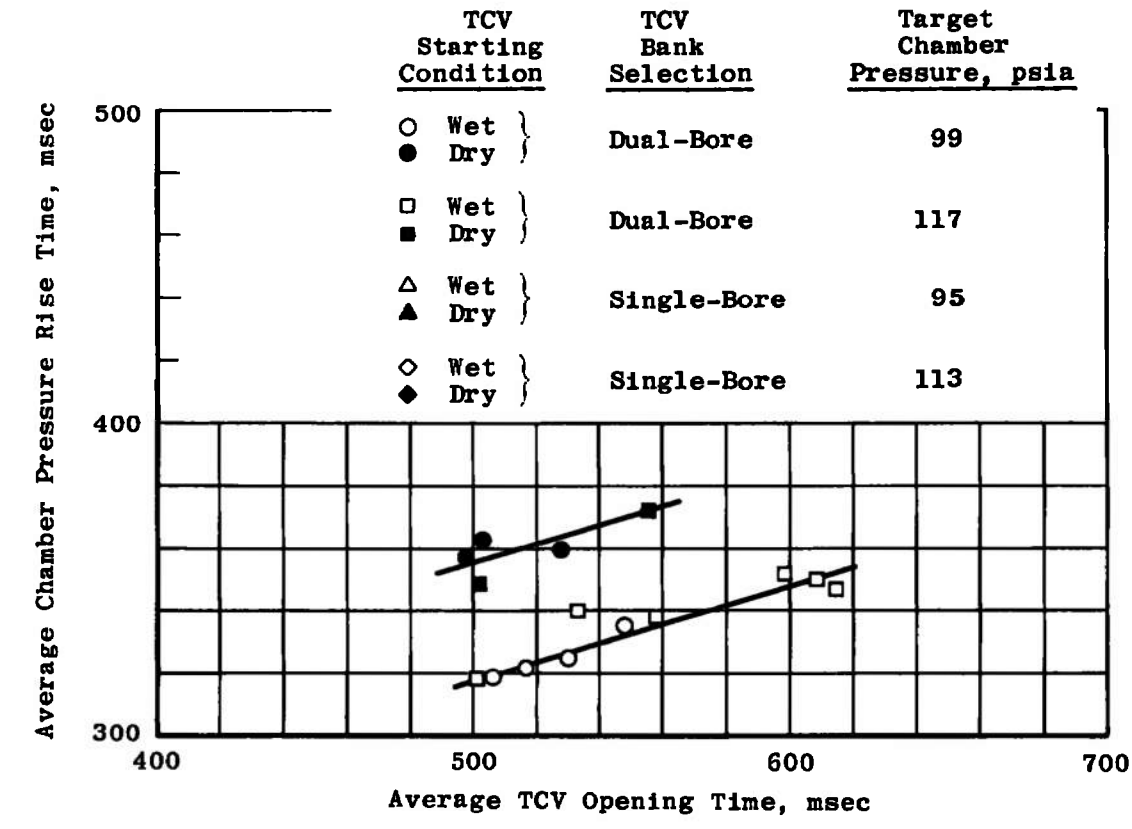

a. Dual-Bore Starts

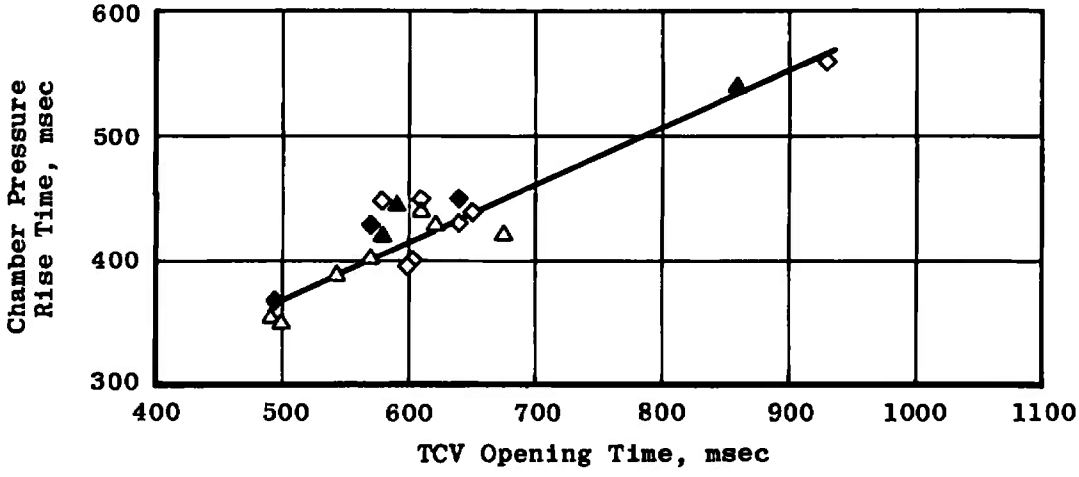

b. Single-Bore Starts

Fig. 14 Chamber Pressure Rise Time as a Function of TCV Opening Time

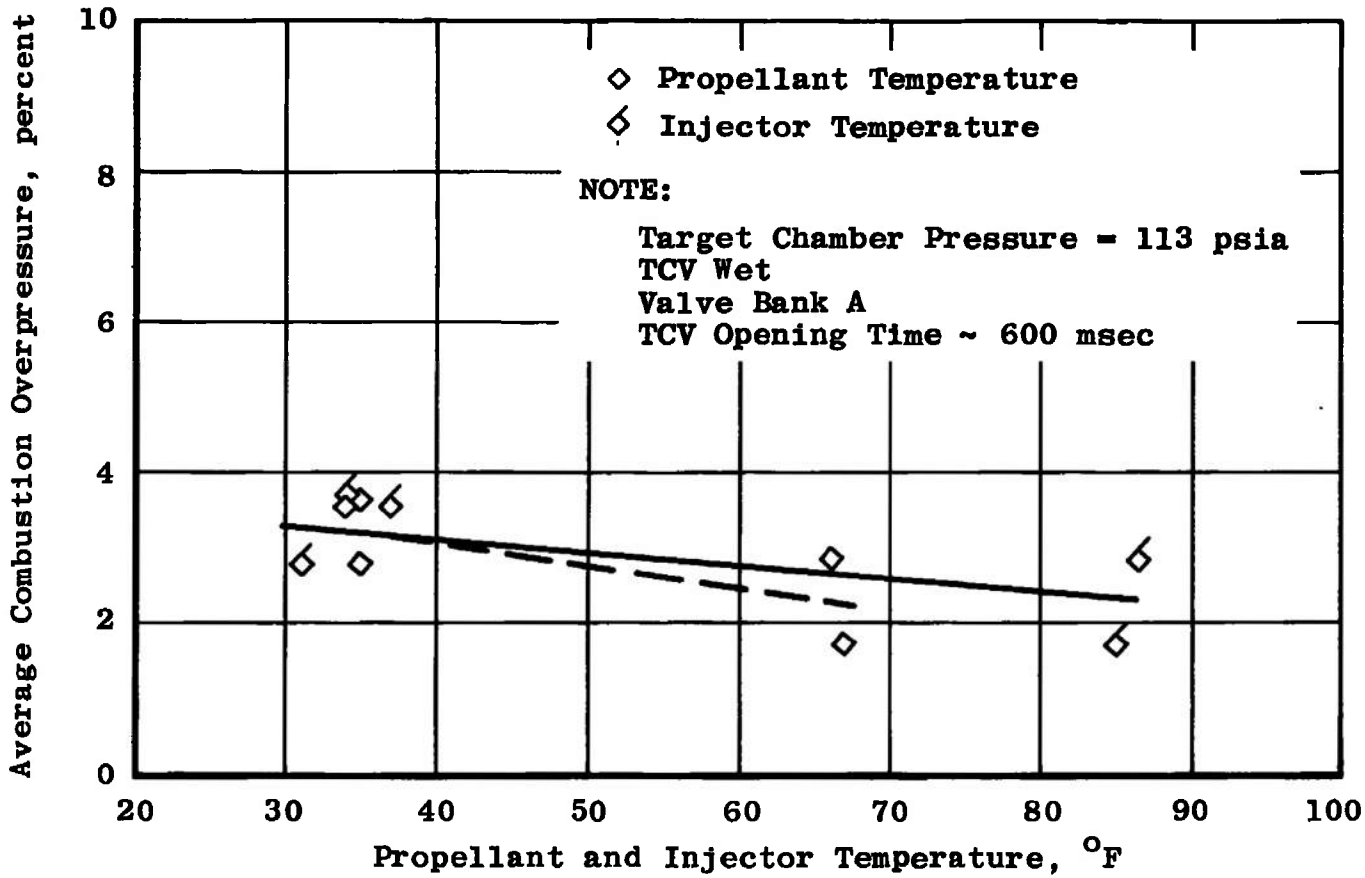

Fig. 15 Average Combution Overpressure as a Function of Propellant and Injector Temperature

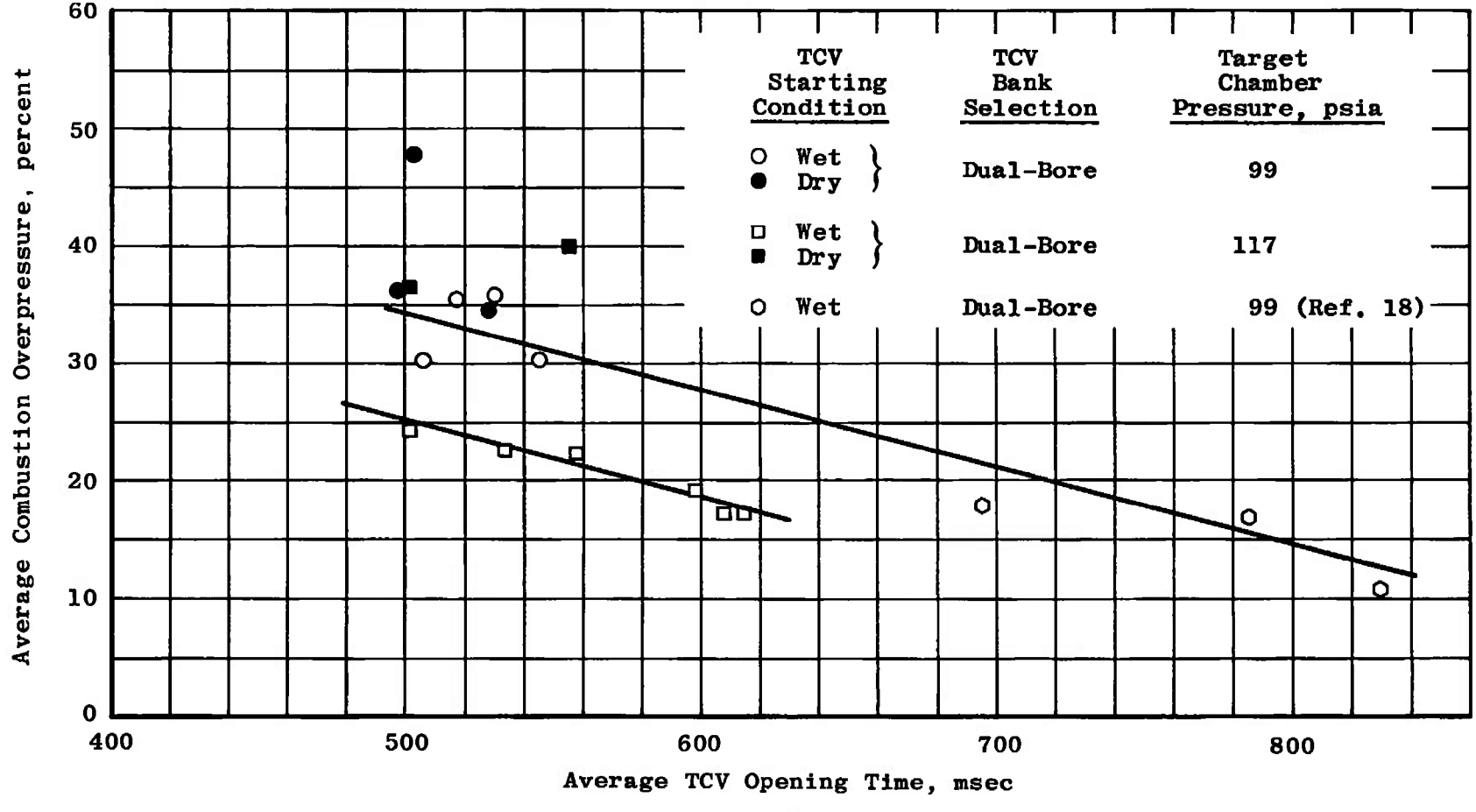

a. Dual-Bore Starts

Fig. 16 Average Combustion Overpressure as a Function of Average TCV Opening Time

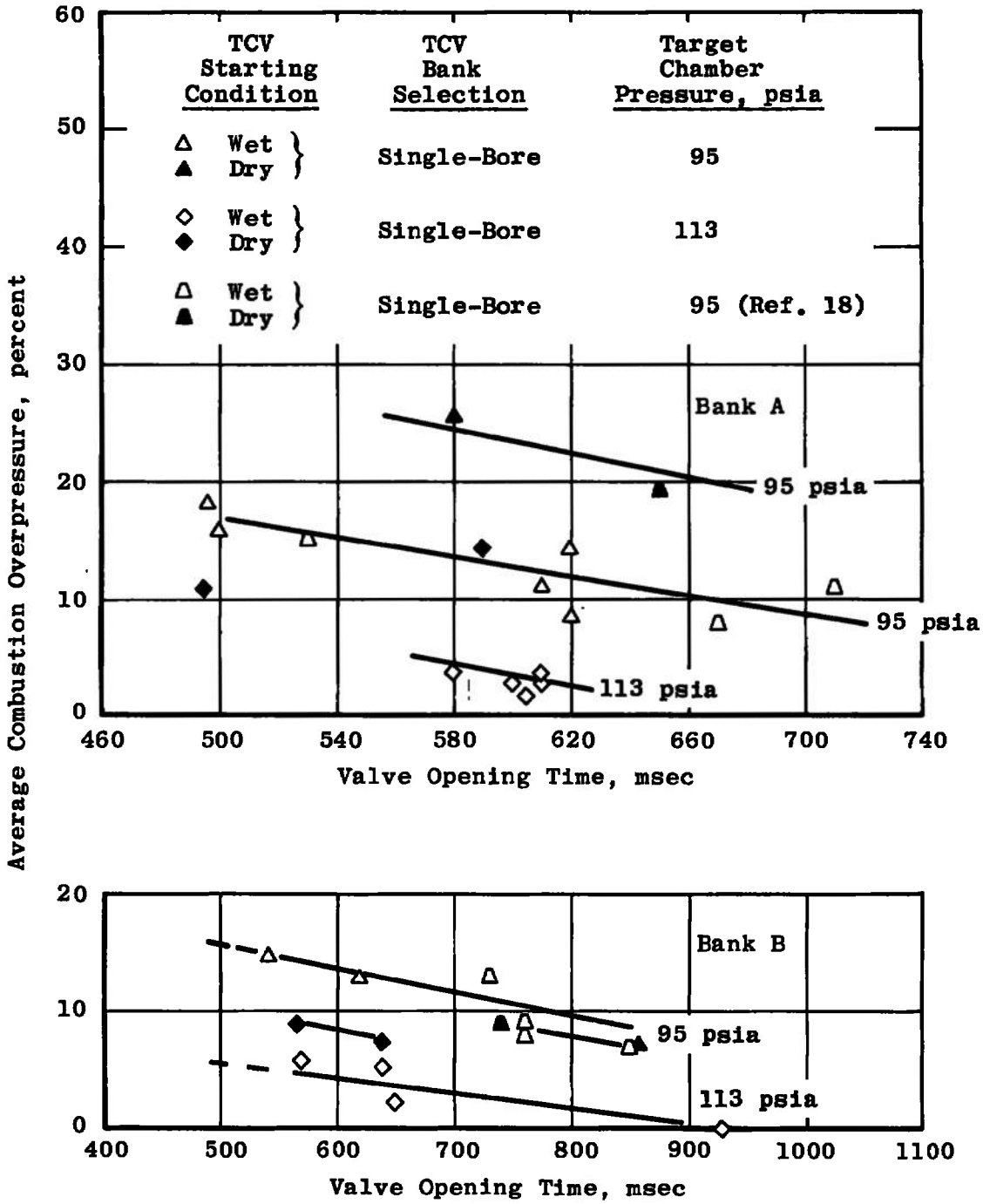

b. Single-Bore Starts, Banks A and B

Fig. 16 Concluded

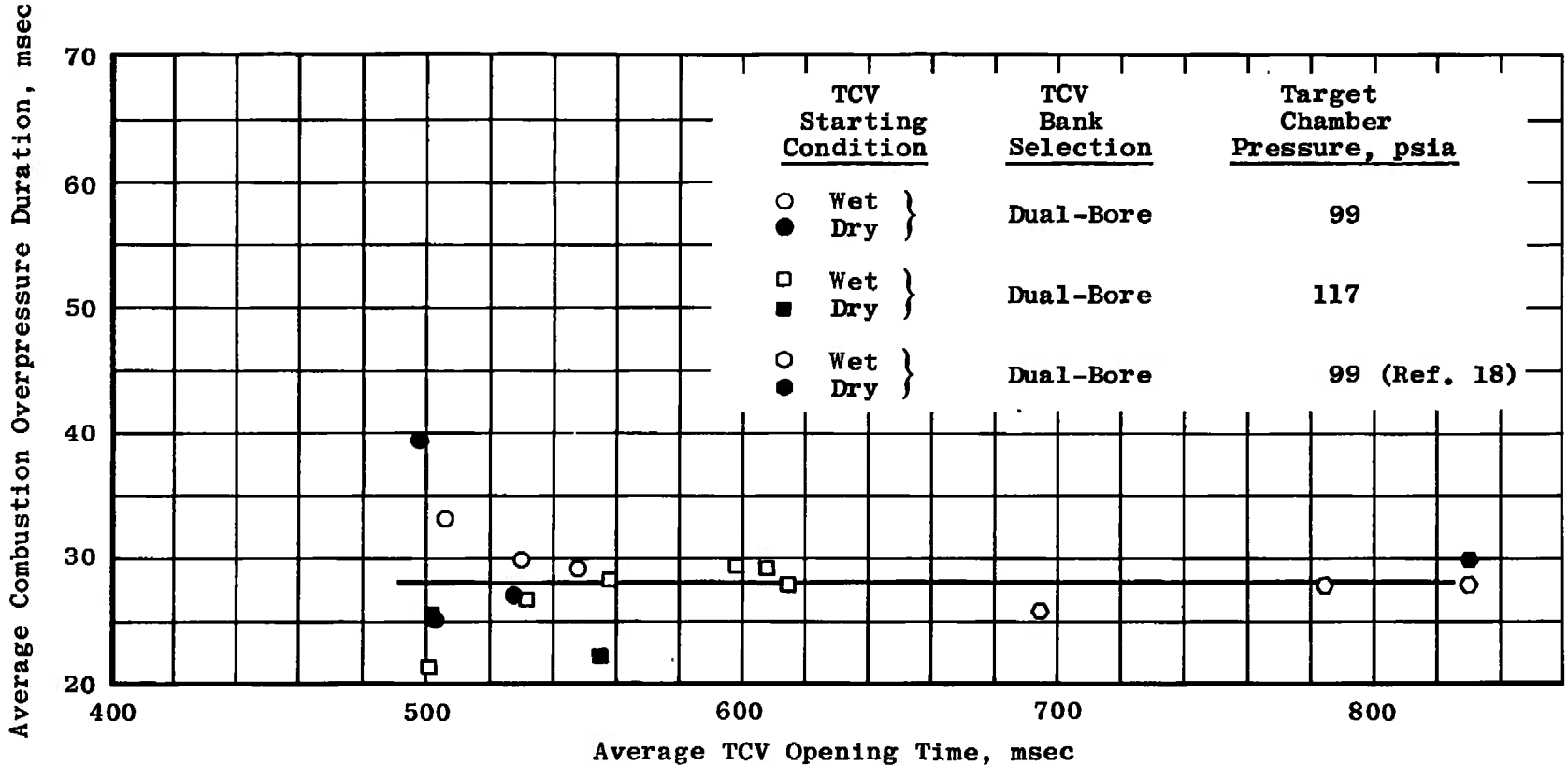

a. Dual-Bore Starts

Fig. 17 Average Combustion Overpressure Duration as a Function of Average TCV Opening Time

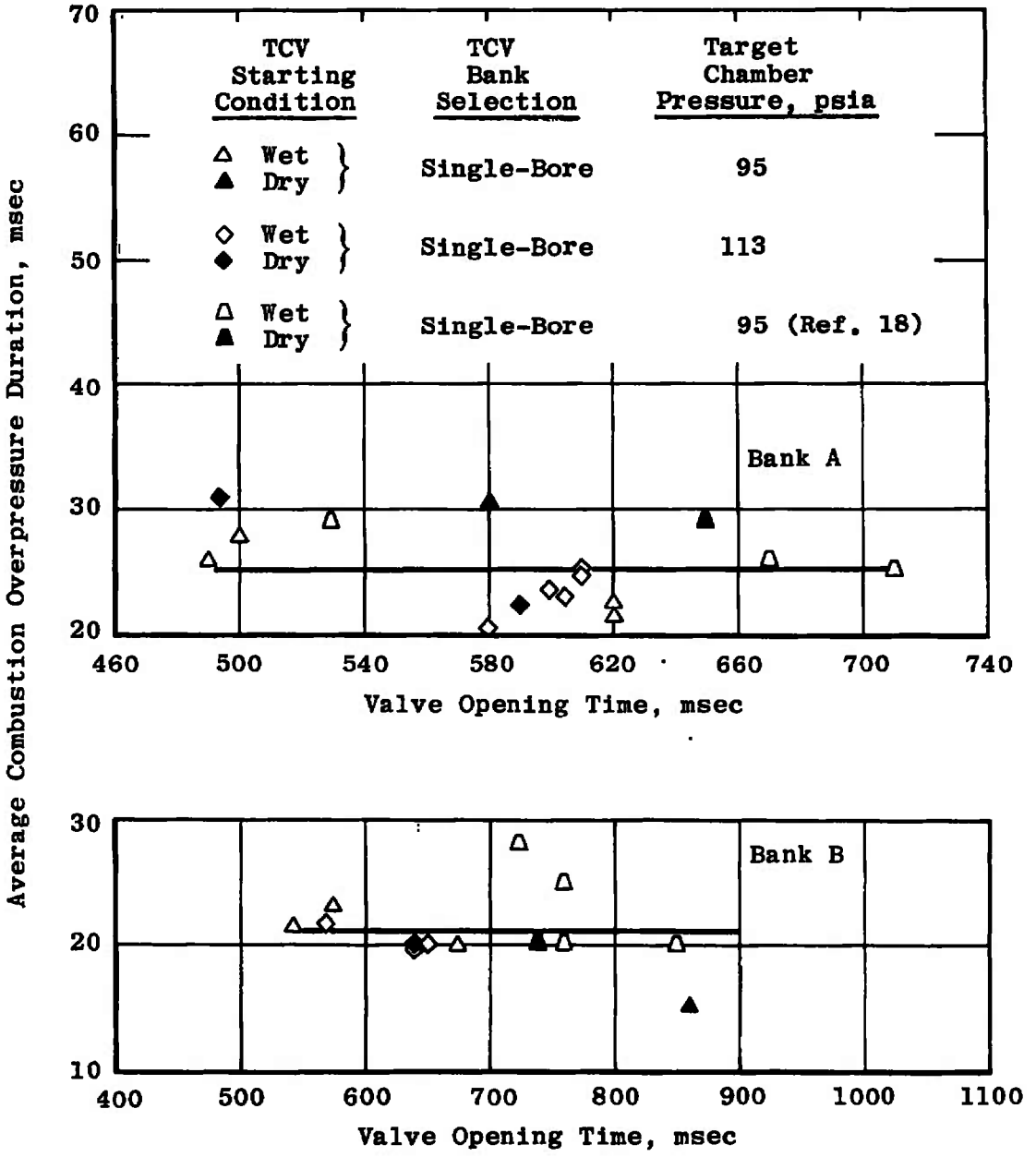

b. Single-Bore Starts, Banks A and B

Fig. 17 Concluded

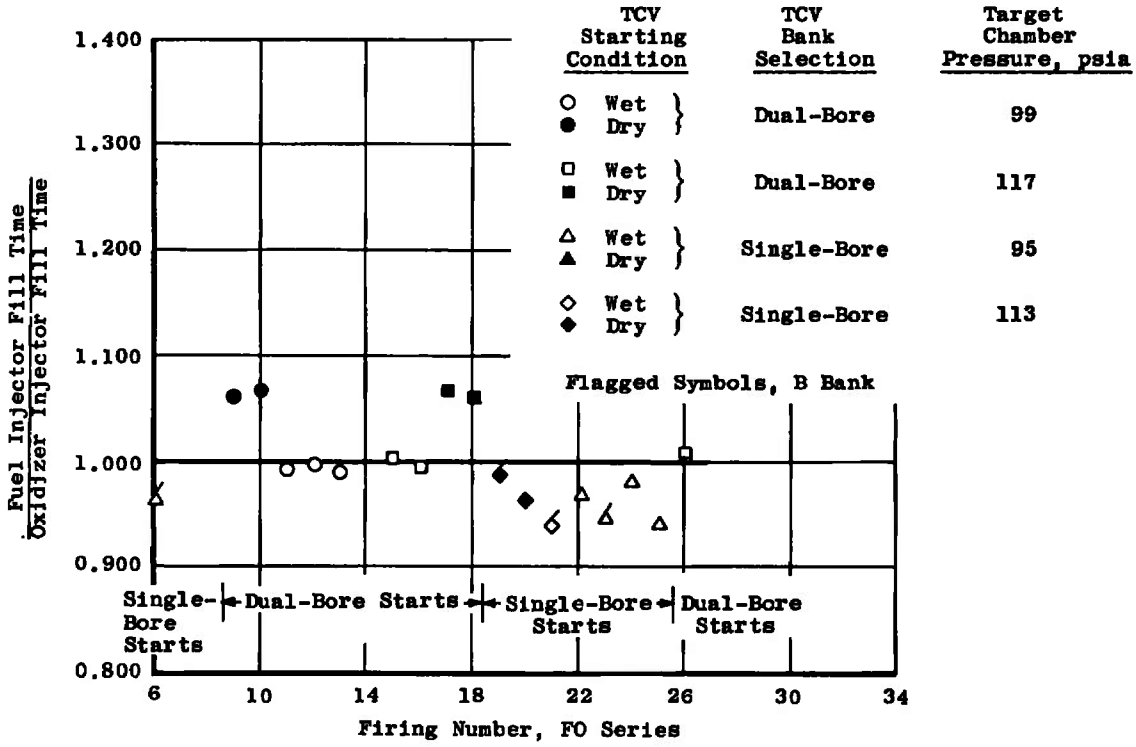

Fig. 18 Ratio of Fuel Injector Fill Time to Oxidizer Injector Fill Time for each Firing

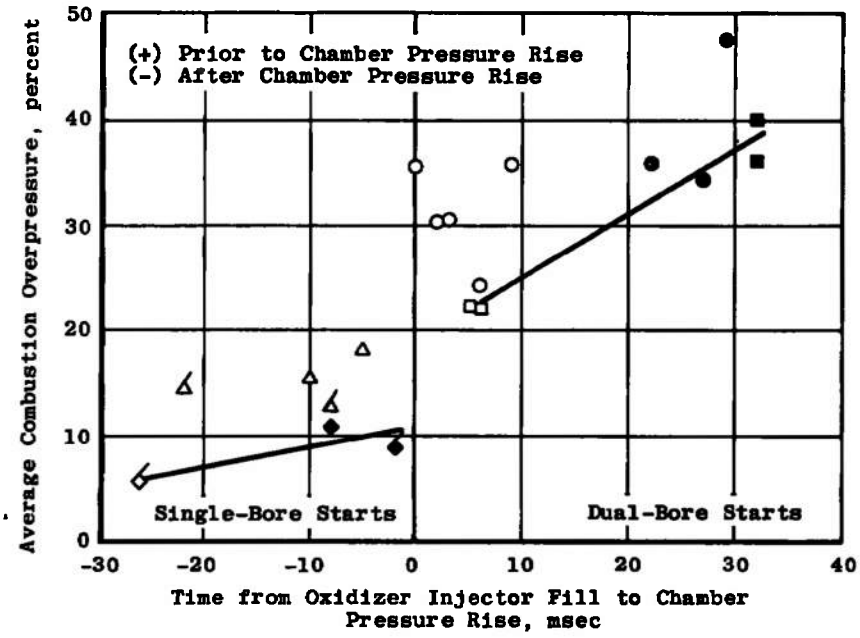

Fig. 19 Average Combustion Overpressure as a Function of the Time from Oxidizer Injector Fill to Chamber Pressure Rise

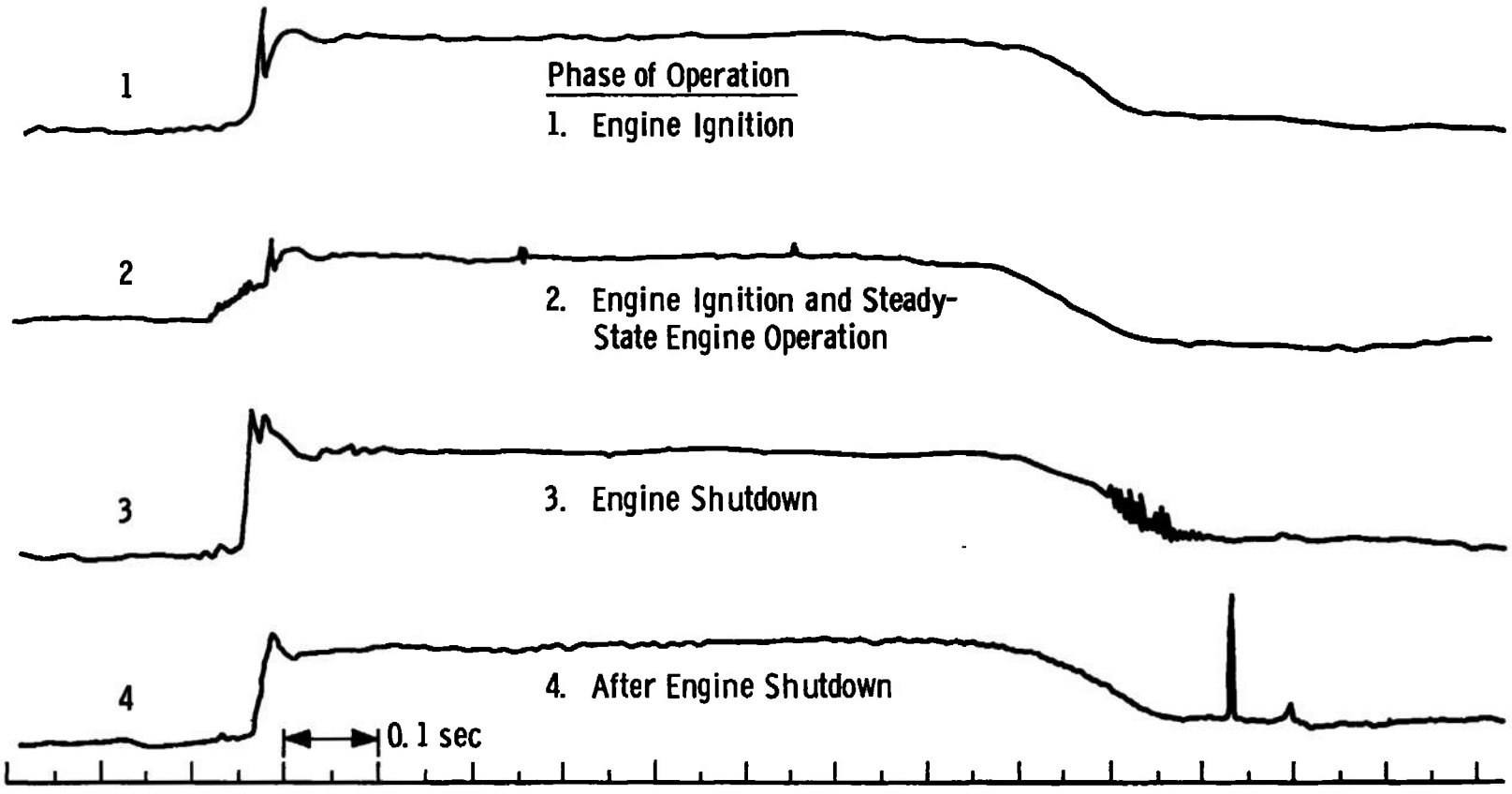

Fig. 20 Analog Traces of Chamber Pressure Spikes

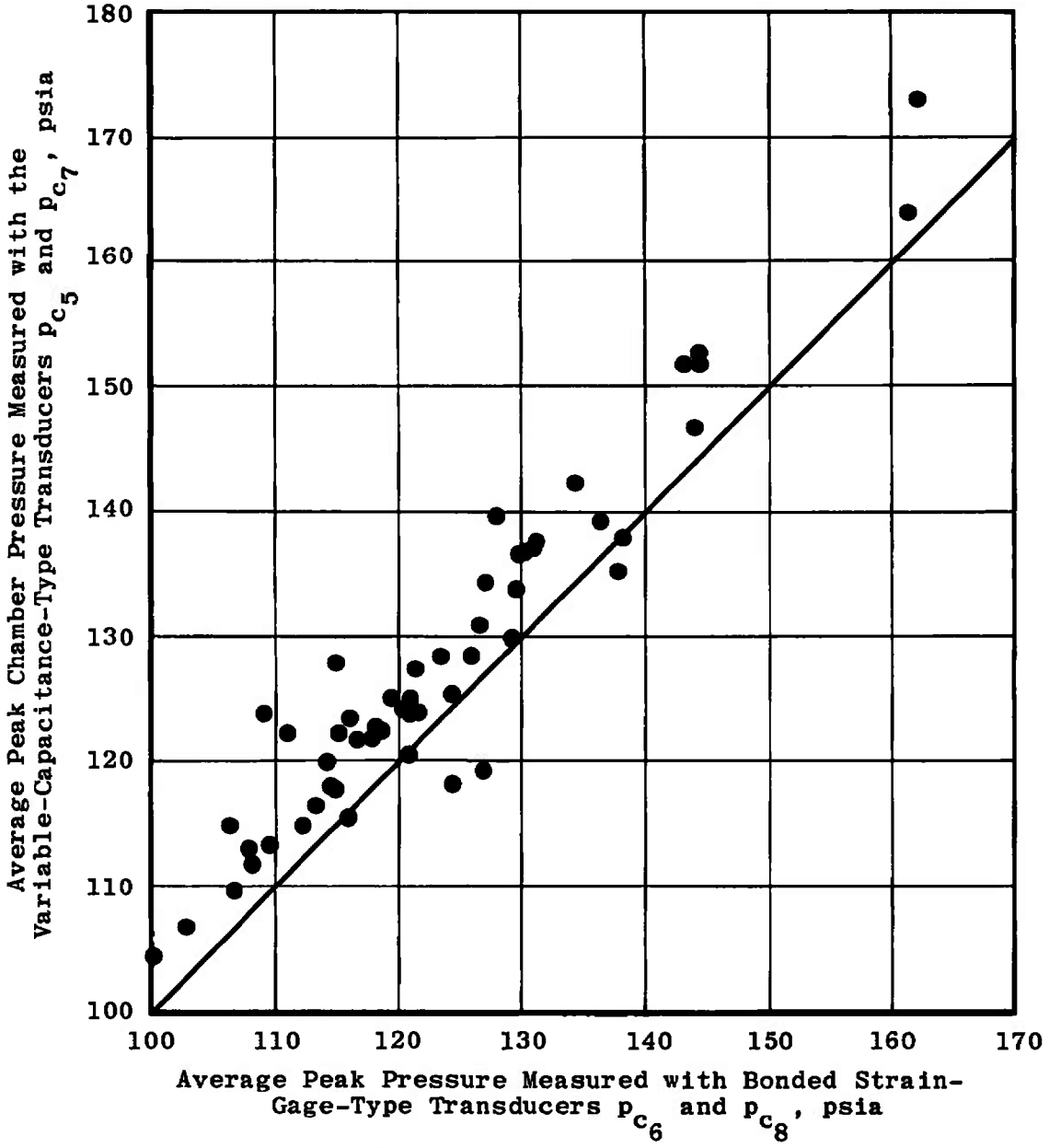

a. Variable-Capacitance-Type Tranducers and Bonded Strain-Gage-Type Tranducers

Fig. 21 Comparison of Chamber Pressure Transducers

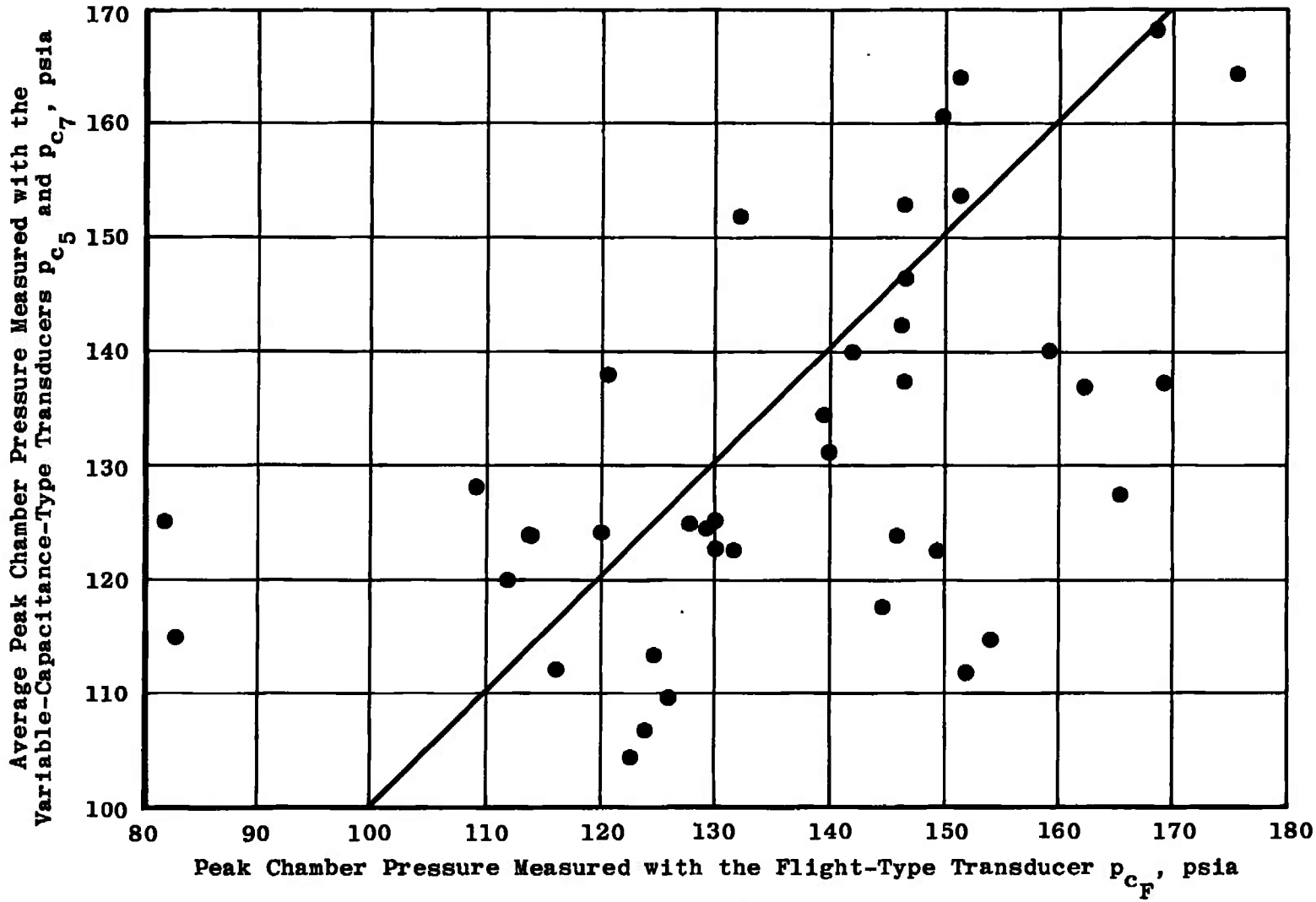

b. Variable-Capacitance-Type Transducers Flight-Type Transducer

Fig. 21 Continued

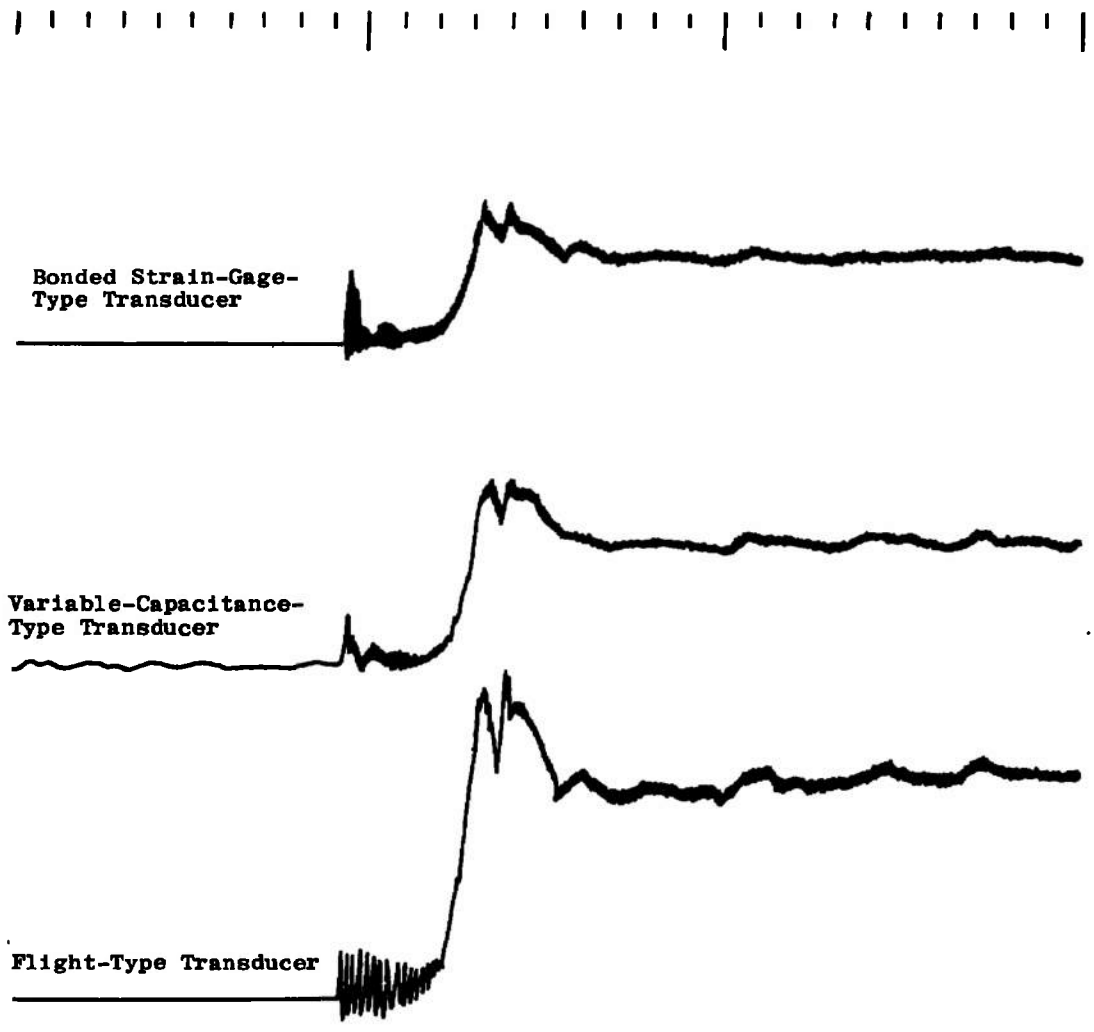

NOTE: The span of the flight-type transducer trace is larger than the span for the other two transducers.

c. Response Time

Fig. 21 Concluded

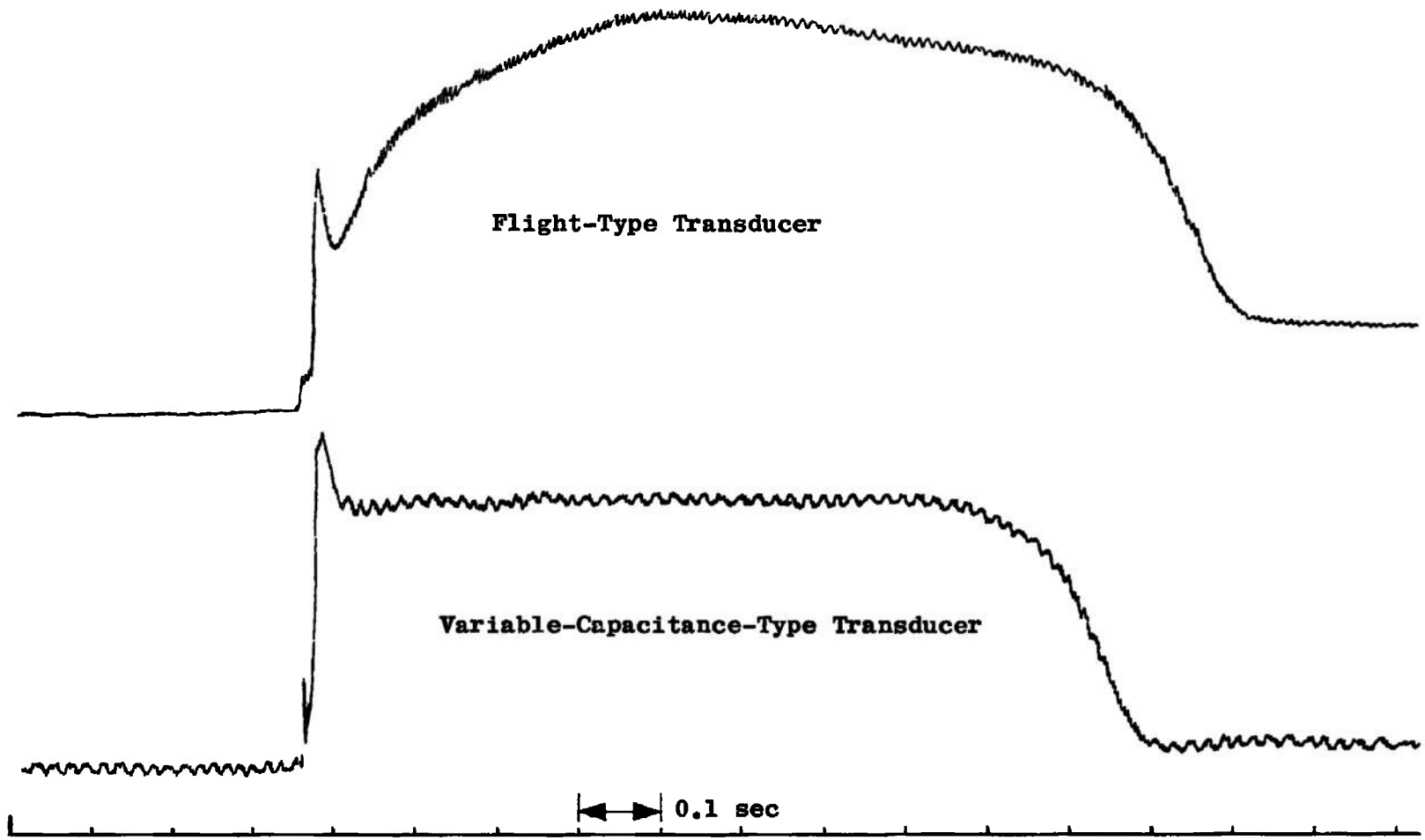

Fig. 22 Comparison of Flight-Type and Variable-Capacitance-Type Transducer Chamber Pressure Data

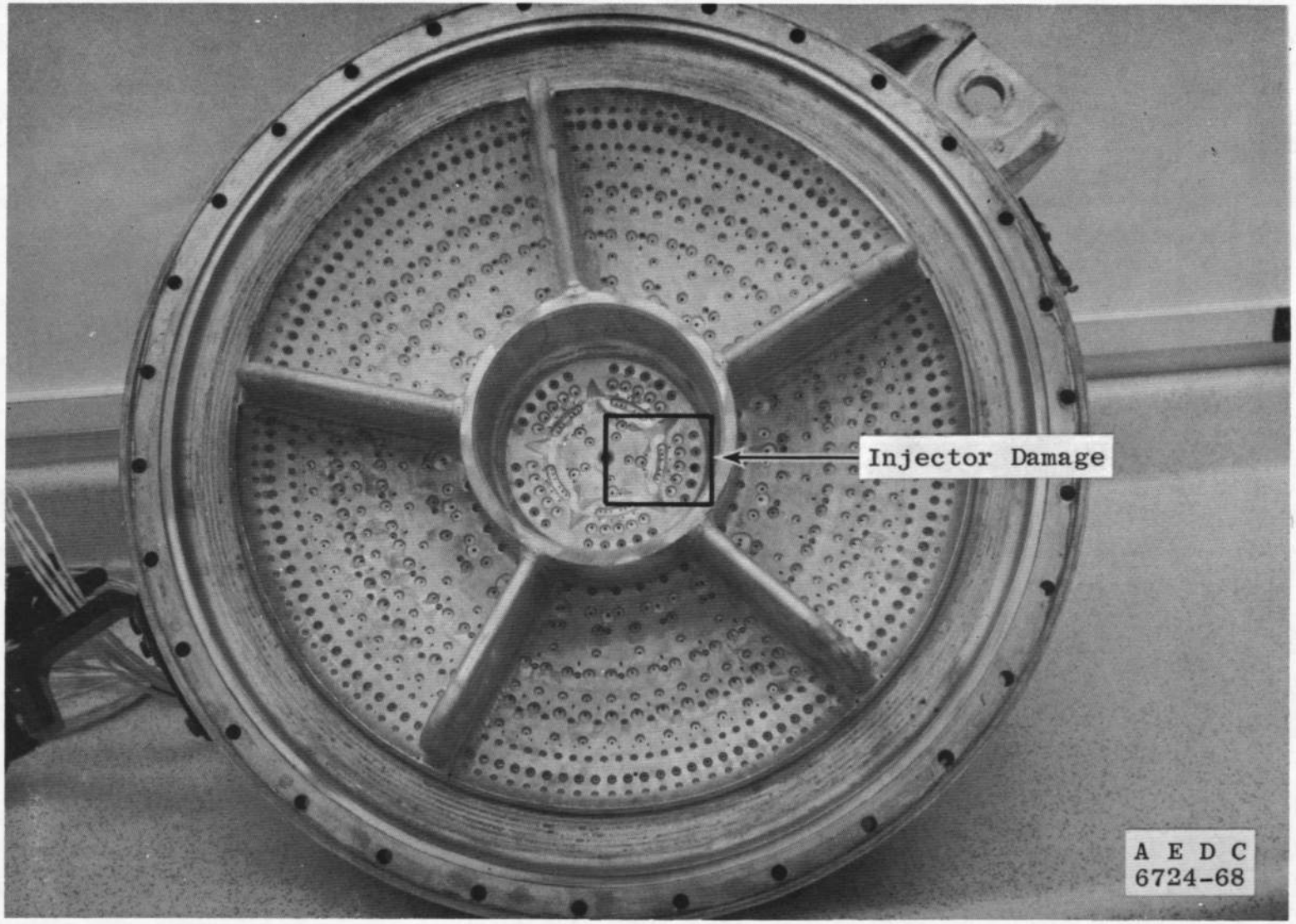

a. Location

Fig. 23 Engine Injector Damage

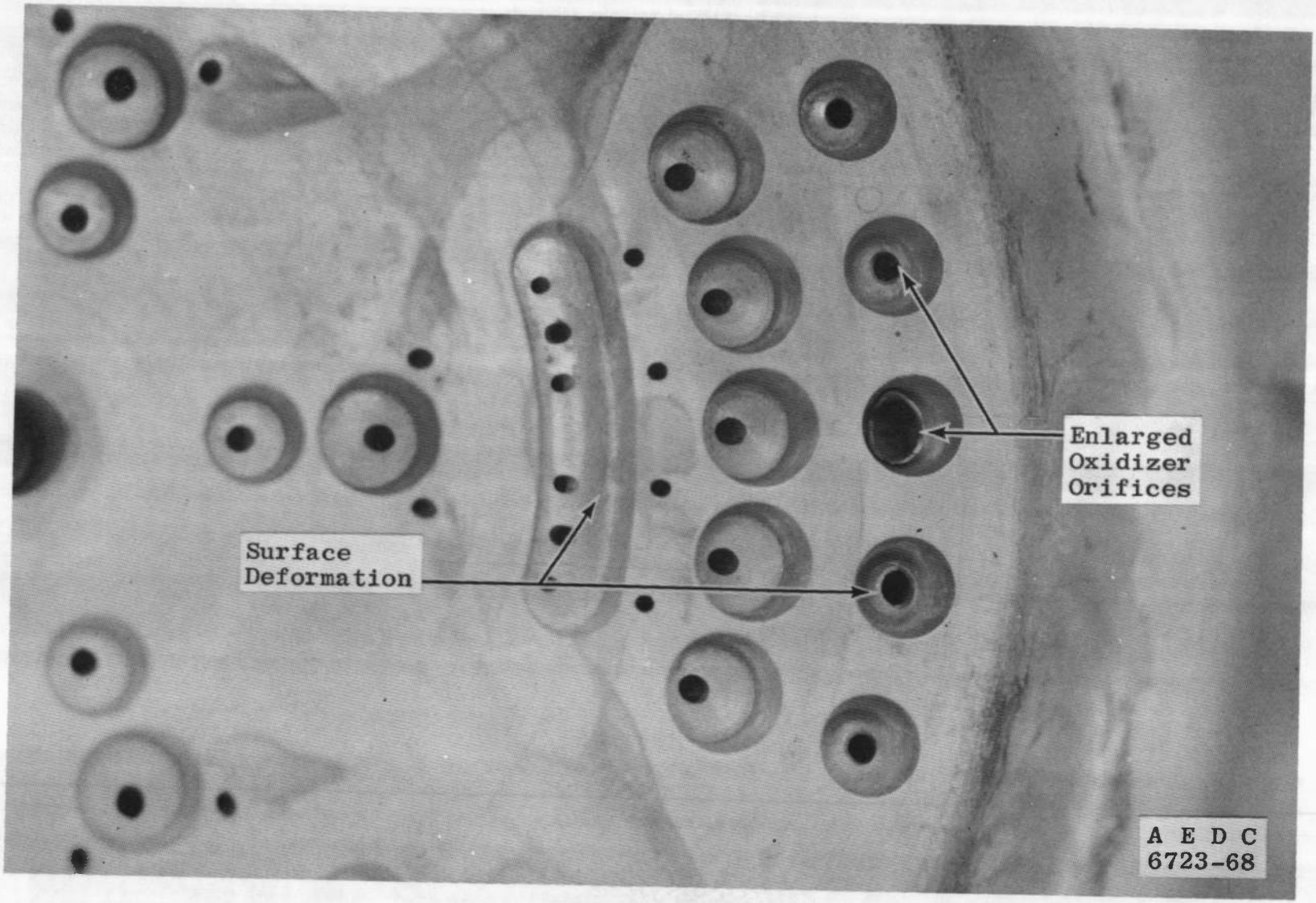

b. Close-up View

Fig. 23 Concluded

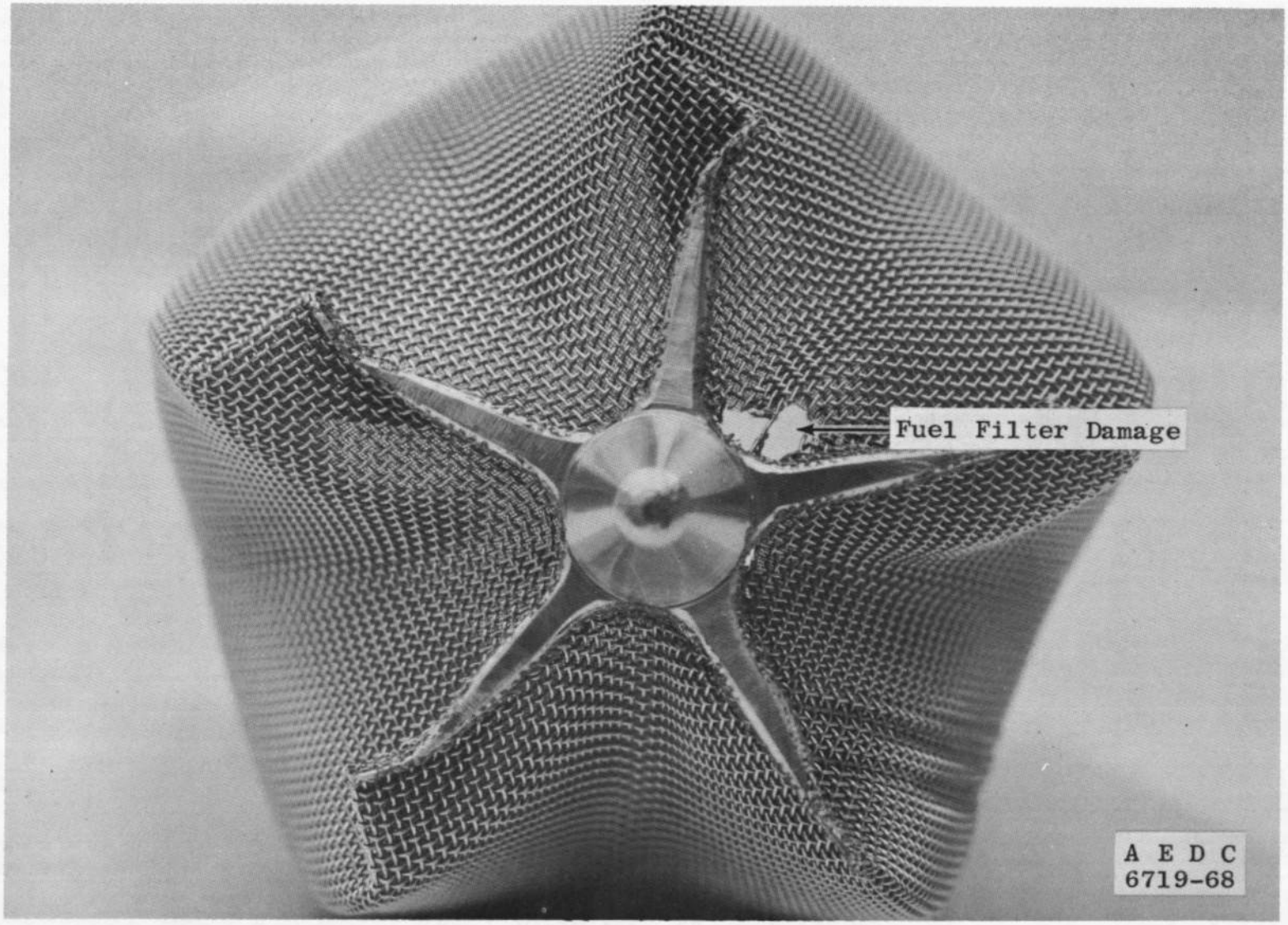

Fig. 24 Fuel Interface Filter Damage

TABLE I
TEST SUMMARY, TEST PERIODS FM AND FN

	Firing No.	Chamber Pressure, p_{c8}, psia	TCV Temperature, °F	Propellant Temperature, °F	Injector Temperature, °F	TCV Bank Selection	TCV Starting Condition	TCV Actuator Temperature, °F	TCV Opening Time, sec	
									Controlling Valve	
									Bank A Valve Set 1	Bank B Valve Set 4
					Test Period FM					
	01	95.2	35	32	39	A	Dry	33	0.580	
	02	95.2	31	31	33	B	↓	30		0.860
*	03	95.2	30	32	35	AB	↓	25	0.620	0.910
	04	96.5	28	31	35	A	Wet	27	0.610	
	05	95.2	26	31	38	A	↓	26	0.620	
	06	95.2	26	31	39	A	↓	26	0.620	
*	07	100.3	25	30	39	AB	↓	25	0.610	0.850
*	08	99.0	24	31	39	AB	↓	25	0.630	0.910
*	09	100.4	25	31	40	AB	↓	25	0.610	0.880
*	10	99.1	26	32	38	AB	Dry	26	0.590	0.850
*	11	99.1	27	31	39	AB	↓	25	0.610	0.910
*	12	96.5	28	31	33	AB	↓	25	0.590	0.910
	13	111.9	29	35	34	A	Wet	25	0.610	
	14	111.9	30	35	31	A	↓	30	0.610	
	15	111.9	30	34	37	A	↓	24	0.580	
	16	109.3	26	31	38	B	↓	25		0.930
*	17	117.0	26	31	37	AB	↓	25	0.630	0.965
*	18	117.0	26	30	38	AB	↓	25	0.630	0.965
*	19	117.0	26	30	35	AB	↓	25	0.620	0.960
					Test Period FN					
	01	112.6	64	70	80	A	Dry	--	0.590	
	02	115.2	59	67	85	A	Wet	--	0.605	
	03	113.9	62	66	87	A	Wet	--	0.600	
	04	113.9	55	66	90	B	Dry	--		0.640
	05	113.9	58	65	96	B	Wet	--		0.640
	06	115.2	52	64	94	B	↓	--		0.650
	07	119.1	55	65	95	AB	↓	--	0.565	0.650
	08	119.1	58	65	100	AB	↓	--	0.590	0.640
	09	117.8	57	65	97	AB	↓	--	0.570	0.625

*Improper TCV Operation

TABLE II
TEST SUMMARY, TEST PERIOD FO

	Firing No.	Chamber Pressure, p_{c8}, psia	TCV Temperature, °F	Propellant Temperature, °F	Injector Temperature, °F	TCV Bank Selection	TCV Starting Condition	TCV Actuator Temperature, °F	TCV Opening Time, sec	
									Controlling Valve	
									Bank A Valve Set 1	Bank B Valve Set 4
*	01	99.7	39	30	26	AB	Dry	43	0.530	0.860
*	02	97.8	28	32	27	AB	Dry	41	0.540	0.925
*	03	97.8	36	25	40	AB	Wet	43	0.560	0.960
*	04	97.8	34	28	38	AB	↓	46	0.575	0.920
*	05	97.8	30	28	40	AB	↓	44	0.570	0.850
*	06	95.9	55	32	50	B	↓	62		0.675
	07	97.8	67	62	58	AB	Dry	59	0.475	0.521
	08	95.9	69	61	78	AB	Wet	60	0.490	0.543
	09	103.0	63	52	47	AB	Dry	78	0.495	0.560
	10	103.0	61	48	87	AB	Dry	65	0.473	0.532
	11	101.0	62	50	78	AB	Wet	70	0.473	0.539
	12	101.0	66	52	95	AB	↓	73	0.520	0.540
	13	103.0	67	52	98	AB	↓	71	0.525	0.570
	14	117.3	70	54	95	AB	↓	72	0.540	0.575
	15	119.7	69	54	99	AB	↓	73	0.505	0.560
	16	118.1	63	53	82	AB	↓	68	0.520	0.595
	17	118.1	67	54	48	AB	Dry	65	0.520	0.590
	18	116.9	68	--	--	AB	↓	65	0.473	0.528
	19	109.3	68	54	160	B	↓	65		0.567
	20	109.3	74	60	140	A	↓	65	0.494	
	21	111.2	73	62	--	B	Wet	64		0.570
	22	92.0	72	63	121	A	↓	65	0.500	
	23	94.0	72	64	120	B	↓	65		0.575
	24	95.1	72	64	113	A	↓	65	0.490	
	25	93.2	71	64	113	B	↓	65		0.543
	26	116.9	70	64	114	AB	↓	65	0.455	0.546

*Improper TCV Operation

TABLE III
COMBUSTION OVERPRESSURE DATA

Firing No.	P_{c_9}				P_{c_8}				P_{c_7}				P_{c_4}				P_{cF}
	Peak Value, psia	Chamber Pressure, psia	Percent Overpressure	Overpressure Duration, msec	Peak Value, psia	Chamber Pressure, psia	Percent Overpressure	Overpressure Duration, msec	Peak Value, psia	Chamber Pressure, psia	Percent Overpressure	Overpressure Durstion, msec	Peak Value, psia	Chamber Preesure, psia	Percent Overpressure	Overpressure Duration, msec	Peak Value, psia
Test Period FM																	
01	119.5	95.2	25.9	32	117.6	94.9	23.9	31	122.5	99.4	27.0	30	107.9	82.0	31.4	26	131.1
02	100.3	95.2	5.4	12	98.7	92.9	8.3	15	104.3	95.2	9.6	16	89.0	84.3	5.5	18	123.7
03	124.8	95.2	30.9	32	---	---	---	30	125.1	100.4	24.5	33	113.5	84.0	35.1	31	129.1
04	109.0	96.6	11.9	25	106.0	95.8	10.9	23	109.5	99.0	10.6	23	95.4	94.0	13.5	23	124.1
05	103.4	98.2	9.8	18	103.1	84.3	9.2	23	109.8	99.0	7.9	25	95.4	81.8	16.7	22	124.1
06	108.5	95.2	14.0	21	107.4	94.4	13.8	21	112.1	97.7	14.7	22	98.9	84.0	18.9	22	118.1
07	123.4	100.3	23.0	27	120.5	97.3	23.8	26	123.8	101.7	23.0	21	104.5	86.3	21.1	24	149.1
09	122.1	99.0	23.0	30	120.5	97.8	23.2	26	125.1	101.7	23.0	29	109.0	86.3	26.3	26	130.1
09	120.8	100.4	20.4	26	118.2	97.3	21.5	26	125.1	101.7	18.0	24	109.0	99.3	26.3	26	80.0
10	114.4	99.1	15.5	25	---	97.3	---	23	119.9	101.6	23.3	24	111.3	86.3	26.9	26	112.1
11	122.1	99.1	23.2	23	119.8	97.3	23.0	24	123.8	100.4	26.0	23	113.5	84.0	35.2	25	114.1
12	119.3	98.5	22.6	25	117.8	100.3	17.4	25	121.7	103.0	19.2	25	104.3	95.0	22.8	25	121.8
13	115.8	111.9	3.5	26	117.8	112.0	5.2	25	121.7	118.1	2.2	25	105.9	96.3	10.0	25	---
14	115.9	111.9	3.5	28	114.9	112.0	2.6	22	121.7	119.1	2.2	26	102.7	96.3	6.8	22	138.6
15	115.8	111.9	3.5	19	116.3	112.0	3.9	20	123.1	118.1	3.3	20	105.9	97.7	8.2	20	---
16	---	109.3	---	---	---	112.0	---	---	---	---	---	---	---	93.1	---	---	119.4
17	129.9	117.0	11.0	28	---	---	---	29	136.4	121.7	12.1	28	110.7	94.7	17.0	28	122.9
18	129.9	117.0	11.0	26	129.4	116.3	11.2	28	133.8	121.7	9.9	26	112.3	99.5	12.9	28	143.3
19	122.9	117.0	4.4	28	125.0	116.3	7.5	26	129.4	120.4	6.8	30	109.1	99.8	9.7	28	125.8
Test Period FN																	
01	130.7	112.6	16.1	25	122.0	106.2	14.8	22	126.4	115.1	11.9	22	129.3	106.9	16.1	22	125.0
02	116.8	115.2	1.1	25	110.5	107.6	2.7	23	116.4	115.1	1.2	24	110.2	103.7	6.3	23	120.2
03	119.1	113.9	4.5	24	110.5	109.1	0.9	23	117.7	113.7	3.5	25	113.4	106.9	8.1	25	120.2
04	123.0	113.9	7.9	20	119.1	109.1	9.7	20	120.4	113.7	5.9	22	111.7	101.7	9.8	20	145.8
05	120.4	113.9	5.7	20	---	110.8	---	16	119.1	113.7	4.7	20	116.8	106.9	9.1	22	---
06	117.6	115.2	2.2	20	114.8	110.5	3.9	18	115.1	113.7	1.2	22	110.1	101.7	8.2	22	---
07	139.8	119.1	17.4	28	133.5	113.4	17.7	29	139.1	119.1	16.9	30	132.8	109.9	25.4	29	125.9
08	141.1	119.1	18.5	28	134.9	113.4	18.9	30	135.1	117.7	14.8	27	129.5	110.2	17.5	30	144.3
09	141.1	117.6	19.8	30	134.8	113.4	18.9	30	137.8	119.4	18.4	29	129.5	106.9	21.1	30	142.0

TABLE III (Continued)

Firing No.	P_{c_9}				P_{c_8}				P_{c_5}				P_{c_7}				P_{c_F}	P_{c_K}
	Peak Value, psia	Chamber Pressure, psia	Percent Overpressure	Overpressure Duration, msec	Peak Value, psia	Chamber Pressure, psia	Percent Ovsrpressure	Overpressure Duration, msec	Peak Value, psia	Chamber Pressure, psia	Percent Overpressure	Overpressure Duration, msec	Peak Value, psia	Chamber Pressure, psia	Percent Overpressurs	Ovsrpressure Durstion, msec	Peak Value, psia	Peak Value, psia
Test Period FO																		
01	120.8	99.7	21.5	25	---	---	---	---	131.1	100.1	31.0	25	117.5	---	---	25	139.5	127.5
02	124.6	87.8	27.5	25	137.9	109.9	35.3	29	140.8	107.2	31.2	23	133.3	101.2	31.7	29	146.8	---
03	111.2	87.8	13.7	30	---	---	---	---	128.3	100.1	28.2	31	119.3	103.8	14.0	29	131.9	---
04	109.3	87.9	12.3	29	---	---	---	---	123.0	104.8	17.4	28	124.3	103.4	20.2	26	120.0	---
05	115.0	97.8	17.8	31	---	---		---	131.1	100.1	31.0	29	124.7	102.5	21.7	32	109.2	---
06	105.4	85.9	10.0	20	107.8	99.0	10.0	19	112.0	97.7	14.9	20	117.5	100.4	17.0	22	92.9	79.8
07	132.3	97.9	35.3	42	124.2	---	---	---	143.0	102.8	38.5	37	139.7	102.5	33.4	39	159.2	150.3
08	130.4	95.9	38.0	36	124.2	---	---	---	138.2	100.1	38.1	31	130.3	98.2	32.7	31	139.5	113.5
09	134.7	103.0	34.8	29	134.0	101.3	32.3	27	147.7	107.2	37.9	27	139.7	102.5	33.4	27	146.5	150.3
10	142.6	103.0	38.5	25	146.4	100.9	45.5	29	157.7	99.2	90.9	25	147.4	100.4	46.8	25	149.5	144.7
11	129.9	101.0	27.5	32	132.0	101.3	30.3	30	141.1	104.9	34.8	36	132.4	102.5	29.2	34	192.2	124.9
12	128.8	101.0	27.5	29	134.0	101.3	32.3	29	143.0	100.1	42.9	32	132.4	102.5	29.2	30	120.8	130.5
13	130.7	103.0	29.9	30	130.7	103.2	26.8	28	141.5	105.9	33.7	29	132.4	99.3	34.7	29	199.2	136.2
14	126.8	117.3	9.1	---	---	---	---	---	133.4	119.1	12.0	---	128.1	115.3	11.1	---	138.8	88.3
15	144.8	119.7	20.9	25	---	---	---	---	159.7	123.9	29.9	29	143.4	121.7	17.9	29	132.1	150.3
16	144.2	119.1	22.1	32	---	114.4	---	28	135.9	119.1	14.0	27	157.2	120.5	30.5	29	146.5	133.3
17	162.2	118.1	37.3	22	---	114.4	---	23	185.1	118.0	39.9	20	170.8	119.9	42.9	24	189.5	187.4
18	155.3	118.9	32.8	25	187.2	119.3	41.3	26	187.5	120.3	38.2	26	160.6	121.3	32.4	25	175.6	181.7
19	124.6	109.3	14.0	---	---	108.8	---	---	---	113.2		---	119.3	114.0	3.9	---	---	---
20	119.8	109.3	9.9	30	124.2	111.7	11.2	31	130.7	114.2	14.4	32	123.9	113.8	9.1	31	195.3	99.3
21	119.9	111.2	8.9	20	---	111.7	---	24	120.7	115.8	4.4	22	123.9	116.2	6.9	20	149.8	105.0
22	107.4	92.0	16.7	28	112.4	84.6	14.2	27	---	---	---	---	113.2	97.0	18.7	28	124.9	---
23	---	94.0	---	25	---	97.4	---	23	---	---	---	---	---	100.4	---	19	---	---
24	110.4	85.1	18.1	28	114.4	94.8	20.7	23	---	---	---	---	114.9	97.8	17.5	25	154.2	104.4
25	108.5	83.2	19.4	22	---	94.7	---	22	---	---	---	---	111.9	99.1	12.9	20	152.1	86.4
26	139.9	116.8	19.7	18	146.4	117.0	25.1	20	---	---	---	21	151.6	118.3	29.1	26	---	157.7

TABLE III (Concluded)

Test Period FO						
Firing No.	P_{c3}			P_{c4}		
	Peak Value, psia	Chamber Pressure, psia	Percent Overpressure	Peak Value, psia	Chamber Pressure, psia	Percent Overpressure
01	98.9	68.1	45.2		78.2	
02	124.3	98.0	26.8	96.8	80.1	20.8
03	123.0	94.5	30.2	91.3	78.2	16.8
04	110.7	97.5	13.5	87.9	80.1	9.7
05	118.6	98.9	19.9	91.6	78.6	16.5
06	114.2	94.5	20.8	78.2	76.4	2.4
07	140.6	94.5	48.8	100.6	83.8	20.0
08	134.0	92.3	45.2	102.4	74.5	37.4
09	139.1	100.0	39.1	107.5	79.0	36.1
10	150.0	95.6	56.9	114.1	77.1	48.0
11	134.8	97.8	37.8	101.6	79.0	28.6
12	137.4	100.4	36.9	99.3	75.2	32.0
13	137.8	98.6	39.8	101.6	76.7	32.5
14	128.2	113.0	13.5	97.8	86.5	13.1
15	143.5	119.5	20.1	112.9	90.3	25.0
16	156.5	113.0	38.5	116.6	90.3	29.1
17	167.4	110.5	51.5	127.3	91.2	39.6
18	165.2	113.0	46.2	127.3	92.3	37.9
19	119.5	110.0	8.6	96.9	86.6	11.9
20	123.9	107.8	14.9	96.9	85.5	13.3
21	120.8	109.1	10.7	96.9	87.8	10.4
22	114.3	90.0	27.0	91.2	74.9	21.8
23		89.1			72.2	
24	110.9	89.1	24.5	87.4	72.6	20.4
25	110.9	92.6	19.8	85.5	74.1	15.4
26	152.1	106.5	42.8	116.3	87.4	33.1

TABLE IV
AVERAGE COMBUSTION OVERPRESSURE DATA

Firing No.	Chamber Pressure Value, psia	Average Duration, sec	Average Combustion Overpressure, percent	Firing No.	Chamber Pressure Value, psia	Average Duration, sec	Average Combustion Overpressure, percent
FM-01	95.4	30.3	25.5	FO-01	99.9	25.0	26.3
02	94.4	15.0	7.1	02	102.0	25.0	31.4
03	97.8	32.3	27.7	03	100.6	29.7	18.0
04	97.1	25.0	11.0	04	101.9	26.7	16.6
05	96.2	22.5	8.6	05	100.1	30.7	23.4
06	95.8	21.3	14.2	06	98.0	20.0	12.9
07	99.8	25.8	23.3	07	100.9	39.5	36.1
08	99.5	27.8	23.2	08	98.1	32.7	35.6
09	99.8	25.8	20.0	09	103.5	27.3	34.5
10	99.3	25.0	19.4	10	100.6	25.3	47.9
11	98.9	23.5	23.7	11	102.4	33.0	30.4
12	99.9	24.5	19.4	12	101.2	30.0	36.0
13	114.3	25.0	3.6	13	102.6	29.3	30.5
14	114.3	24.5	2.8	14	117.2	39.3	10.4
15	114.3	20.3	3.6	15	121.7	26.7	22.5
16	112.1	No Over-pressure	---	16	118.3	28.3	22.2
				17	117.5	22.3	40.0
17	119.4	28.0	11.6	18	119.2	25.5	36.4
18	118.3	28.0	10.7	19	111.6	---	8.9
19	117.9	28.5	6.2	20	112.2	31.0	10.9
				21	113.7	21.5	6.0
FN-01	111.3	22.3	14.2	22	94.6	37.7	15.9
02	112.6	23.0	1.7	23	97.3	23.3	
03	112.2	23.5	2.9	24	95.9	25.7	18.1
04	112.2	20.0	7.5	25	95.7	21.3	14.7
05	112.7	19.5	5.2	26	117.4	21.3	24.3
06	113.1	20.0	2.4				
07	117.2	29.3	17.3				
08	116.7	28.0	17.4				
09	115.9	29.5	19.0				

APPENDIX III
DESCRIPTION OF THRUST CHAMBER VALVE (TCV) OPERATION

A physical description of the TCV is included in Section 2.1.4 and Fig. 3 (Appendix I). This appendix is included for the purpose of describing the TCV operational sequences which affected injector fill characteristics.

The four basic types of engine starts were:

1. Dual-bore (A and B), dry
2. Dual-bore (A and B), wet
3. Single-bore (A or B), dry
4. Single-bore (A or B), wet

The two sets of valves in each bank (designated 1 and 2 in bank A and 3 and 4 in bank B) are each operated by a separate actuator. The four actuators were timed such that valve sets 2 and 3 opened earlier than valve sets 1 and 4, respectively, by approximately 10 msec and closed later than sets 1 and 4. The opening times for valve sets 2 and 3 are approximately half that of sets 1 and 4. The effect of this on the starting sequence is that sets 1 and 4 become the controlling valves.

As a result of the flow directions and valve arrangement shown in Fig. 3 and Fig. III-1, sets 1 and 4 each opened an upstream fuel ball and a downstream oxidizer ball, and sets 2 and 3 each opened a downstream fuel and an upstream oxidizer ball.

The prefire valve condition is shown in Step A, Fig. III-1 for both wet and dry starts. Both the fuel and the oxidizer cavities are empty in the dry condition but contain some trapped propellants in the wet condition. In Step B, valve set 2 begins to open first with valve set 1 remaining closed, and the following occur: For the dry start sequence, oxidizer is allowed to flow past the oxidizer valve ball of set 2 to fill the cavity, and no fuel flows since valve set 1 remains closed. For the wet start sequence condition, no oxidizer flow occurs; however, the fuel contained in the valve cavity is released from the cavity through the fuel valve ball of set 2. In Step C, valve set 1 now opens and the following occur: For the dry start sequence, fuel is allowed to pass under control of valve set 1 through the fuel valve ball of set 2 to the injector, and oxidizer is allowed to flow to the injector through the oxidizer valve ball of set 2 but under the control of the oxidizer valve ball of set 1. In the wet condition, fuel is released from the fuel valve ball of set 1 through the fuel valve ball of set 2 forcing the residual fuel from the

cavity into the injector, and oxidizer flows through oxidizer valve ball of set 2 but under the control of the oxidizer valve ball of set 1. In Step D, all valves are full open, and full flow of both fuel and oxidizer is established.

In Fig. III-1, it can be seen that in the wet condition a quantity of both fuel and oxidizer is trapped within the valve, both in the cavity between the valve balls and within the balls; conversely, in the dry condition, both the cavities and balls are void of propellants. The effect of the wet condition on a start is that the volume which must be filled in both oxidizer and fuel manifolds is less than for the dry condition, single or dual bore, and therefore, less time is required to fill both manifolds. However, when operating in the wet condition, dual or single bore, the fuel manifold fills substantially faster than does the oxidizer manifold because the quantity of trapped fuel in the TCV is greater than the quantity of trapped oxidizer. This results in fill time variations as outlined in Section 4.1.[1]

One unexplainable event is that, although both manifolds fill slower during single-bore starts than during dual-bore starts, the oxidizer manifold fills substantially slower during single-bore starts than does the fuel manifold, and a fuel lead results as contrasted with an oxidizer lead during dual-bore starts. This effect occurs for both the wet and dry conditions; however, it is more pronounced for the dry condition.

On shutdown, valve set 1 will close before valve set 2 with the following results: on the fuel side, the effect of valve set 2 closing last will tend to vent the cavity between the balls; however, on the oxidizer side, valve set 1 will have already stopped flow when valve set 2 closes, and the cavity will be full. This sequence provides the wet start condition for the next firing as shown in Step A, Fig. III-1.

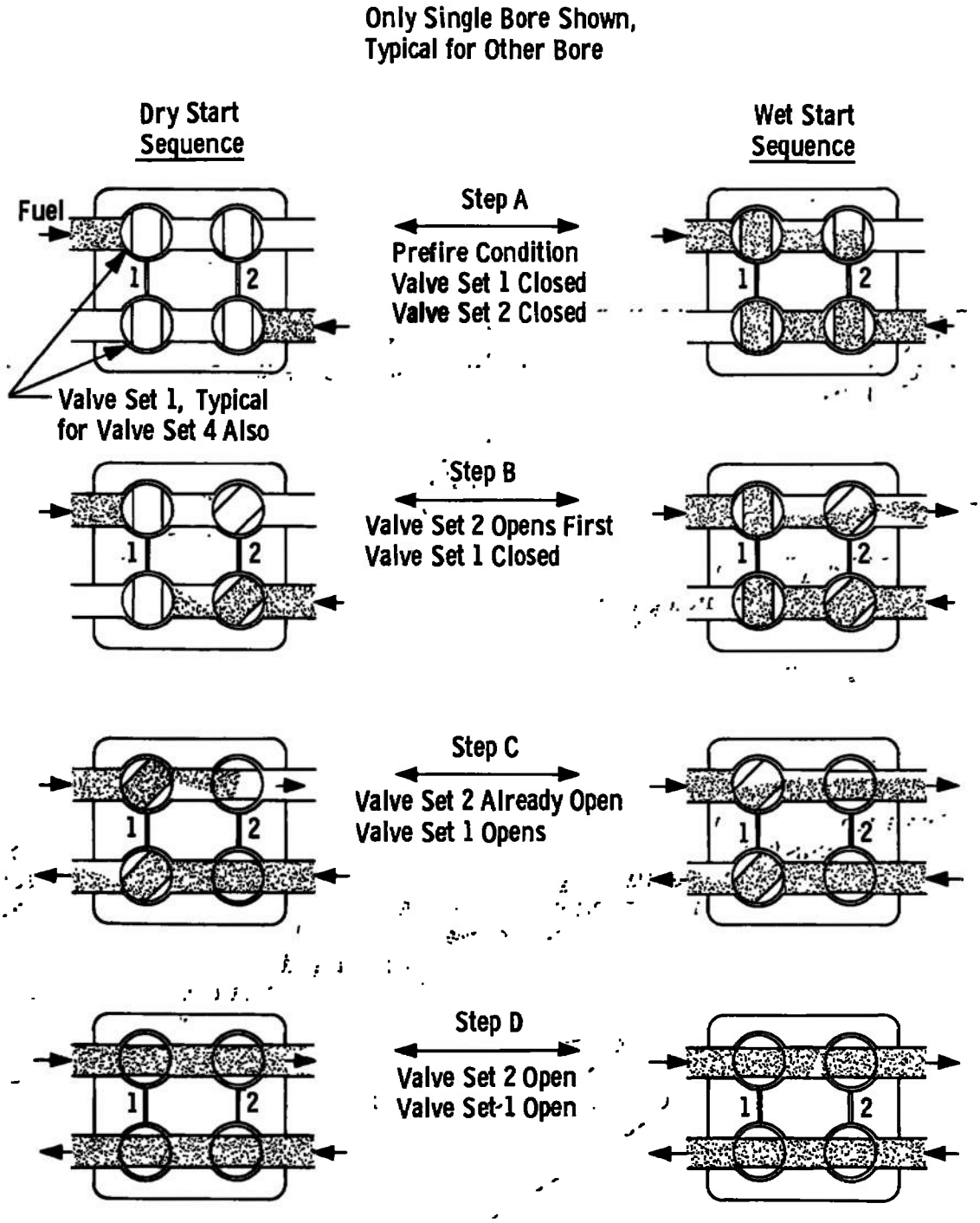

Fig. III-1 Schematic of Thrust Chamber Valve

UNCLASSIFIED

Security Classification

DOCUMENT CONTROL DATA - R & D

(Security classification of title, body of abstract and indexing annotation must be entered when the overall report is classified)

1. ORIGINATING ACTIVITY (Corporate author)
Arnold Engineering Development Center
ARO, Inc., Operating Contractor
Arnold Air Force Station, Tennessee 37389

2a. REPORT SECURITY CLASSIFICATION
UNCLASSIFIED

2b. GROUP
N/A

3. REPORT TITLE
INVESTIGATION OF COMBUSTION OVERPRESSURE DURING IGNITION OF THE APOLLO BLOCK II SPS ENGINE (AJ10-137)(PHASE VI, PART II)

4. DESCRIPTIVE NOTES (Type of report and inclusive dates)
Final Report May 27 to June 28, 1968

5. AUTHOR(S) (First name, middle initial, last name)
R. L. Barebo and R. C. Ansley, ARO, Inc.

This document has been approved for public release; its distribution is unlimited. Per A 4 Letter Dated 27 Jan 23

6. REPORT DATE	7a. TOTAL NO. OF PAGES	7b. NO OF REFS
January 1969	71	18

8a. CONTRACT OR GRANT NO.	9a. ORIGINATOR'S REPORT NUMBER(S)
F40600-69-C-0001	AEDC-TR-68-273
b. PROJECT NO. 9281	
c. Program Area 921E	9b. OTHER REPORT NO(S) (Any other numbers that may be assigned this report) N/A
d.	

10. DISTRIBUTION STATEMENT This document is subject to special export controls and each transmittal to foreign governments or foreign nationals may be made only with prior approval of NASA-MSC (EP-2), Houston, Texas 77058.

11. SUPPLEMENTARY NOTES	12. SPONSORING MILITARY ACTIVITY
Available in DDC.	NASA-MSC (EP-2) Houston, Texas 77058

13. ABSTRACT

An investigation was conducted to determine the magnitude and duration of combustion overpressure during ignition of the Apollo SPS Block II engine. Fifty-four engine starts were made at a pressure altitude of 115,000 ft for a total of 62 sec of firing time. Engine hardware and propellant temperatures were varied from 30 to 70°F but did not influence combustion overpressure. The magnitude of combustion overpressure was affected by propellant injector fill characteristics which were a function of bipropellant valve opening time and target chamber pressure. The overpressure ranged from 0 to 48 percent above the steady-state chamber pressure level for durations ranging from 15 to 39 msec. The overpressure duration was not influenced by the various starting conditions.

This document is subject to special export controls and each transmittal to foreign governments or foreign nationals may be made only with prior approval of NASA-MSC (EP-2), Houston, Texas 77058.

DD FORM 1 NOV 65 1473

UNCLASSIFIED

Security Classification

14. KEY WORDS	LINK A		LINK B		LINK C	
	ROLE	WT	ROLE	WT	ROLE	WT
Apollo SPS Engine						
rocket engines						
liquid propellants						
combustion overpressure						
altitude simulation						

1. Missiles -- Apollo
2 Rocket motors -- AJ10-137
3 " " -- Combustion overpressure
4 " " -- Ignition
5 Combustion overpressures.

16-3

AFSC
Arnold AFS Tenn